NTNU

Norwegian University of
Science and Technology

Optimization of the Resulting Characteristic for Power Amplifiers Using Predistortion

Børge Ellingsen Kristiansen

Master of Science in Communication Technology
Submission date: May 2008
Supervisor: Nils Holte, IET

Norwegian University of Science and Technology
Department of Electronics and Telecommunications

Problem Description

The objective of this thesis is to estimate an optimum resulting nonlinear characteristic for a single carrier transmission system using predistortion, so that the transmitted power is maximized while fulfilling given requirements for the out of band spectrum.

Assignment given: 14. January 2008
Supervisor: Nils Holte, IET

Abstract

Power amplifiers are nonlinear devices that traditionally have been tried linearized by means of predistortion. The nonlinear impact can be identified by sidelobes in the frequency domain. By accepting a certain sidelobe level, this implies that we also accept a somewhat nonlinear characteristic on the resulting cascade of our transmitter. The main question raised in this thesis is: How is the optimal nonlinear cascade that maximizes transmitted power defined when some given out-of-band spectral requirements are fulfilled?

The problem has been limited such that examinations have been done on a single carrier system seen in context to a chosen set of out-of-band spectral requirements. The different nonlinear characteristics have been represented by means of B-splines. Thus, the results obtained are only the best set of parameters in the model utilized, and hence, only a sub-optimal solution to the problem.

Results are presented for different spectral restrictions. Simulations performed suggest that a linear characteristic is the optimal, when restrictions are placed within the sidelobe level close to the mainlobe. When the first sidelobe is allowed to grow unlimited, a parameter set using 2-segments B-spline have proved to give the highest average transmitted power.

Preface

This thesis is the concluding part of my 5-year master degree at the Norwegian University of Science and Technology (NTNU), Department of Electronics and Telecommunications (IET). It is the first major project I have done, and it has given me an insight into how research is done in university context.

I would like to express a special thank to my supervisor, Professor Nils Holte, for answering my questions, as well as pointing out important matters I would never have thought of by myself. Also, I would like to thank my fellow students Ane Sæstad and Tormod Emsell Larsen for giving me valuable feedback on my English and pointing out vague descriptions.

Børge Ellingsen Kristiansen
Trondheim, May 26. 2008

Contents

Preface i

Contents iii

List of Figures v

Abbreviations vii

1 Introduction 1
- 1.1 Motivation . . . 1
- 1.2 Objective . . . 1
- 1.3 Scope and Limitations . . . 2
- 1.4 Methodology . . . 2
- 1.5 Structure . . . 2

2 Background Theory 3
- 2.1 Power Spectral Density . . . 3
  - 2.1.1 The Periodogram Estimate . . . 3
  - 2.1.2 The Averaged Modified Periodogram . . . 4
- 2.2 Modeling Nonlinearities by Means of B-Splines . . . 5
  - 2.2.1 Fixed Weight Coefficients on Nonlinearity . . . 6
  - 2.2.2 Selecting Weight Coefficients with One Degree of Freedom . . . 9
- 2.3 Nonlinear Impact upon a Signal . . . 10
  - 2.3.1 Examination of Nonlinear Impact in the Time Domain . . . 11
  - 2.3.2 Examination of Nonlinear Impact in the Frequency Domain . . . 12

3 Methodology 15
- 3.1 System Model . . . 15
- 3.2 Optimization Criterion . . . 16
- 3.3 Simulation Environment . . . 18
- 3.4 Simulations - A Statistical Approach . . . 19
- 3.5 Confirmation of Simulation Program . . . 20

4 Simulation Results 23
- 4.1 A Simple Mask close to the Mainlobe . . . 23
  - 4.1.1 An Ideally Predistorted System . . . 24
  - 4.1.2 Nonlinear Systems . . . 25

4.1.3 Important Observations . . . 29
4.2 A Simple Mask at 1.7/T . . . 29
4.2.1 An Ideally Predistorted System . . . 29
4.2.2 Nonlinear Systems . . . 30
4.2.3 Important Observations . . . 32
4.3 Restricting the PSD with the BGAN Spectral Mask . . . 33
4.3.1 An Ideally Predistorted System . . . 34
4.3.2 Nonlinear Systems . . . 35
4.3.3 Important Observations . . . 37

5 Conclusions **39**
5.1 Conclusions and Main Findings . . . 39
5.2 Future Work . . . 39

Bibliography **41**

List of Figures

2.1 B-Spline basis functions when utilizing six segments 6
2.2 Comparison of different nonlinearities using constant weight coefficients 9
2.3 Different nonlinearities obtained utilizing a 2-segments nonlinearity, with different accepted values for a_1 11
2.4 Comparison of a distorted and a nondistorted 16-QAM signal 11
2.5 PSDs of the linear addend in a baseband signal (black), the cubic nonlinear addend in a baseband signal (blue) and the quintic nonlinear addend in a baseband signal (green) 13
2.6 The resultant transmitted PSD from a nonlinearity 13

3.1 A basic baseband system model utilizing a nonlinear amplifier and predistortion 15
3.2 The modified transmitter model, where a nonlinear element is inserted, and ideal predistortion is assumed 16
3.3 Constraining the transmitted PSD with a simple spectral mask 17
3.4 Constraining the transmitted PSD with the BGAN spectral mask 18
3.5 Comparison of an acceptable and a non-acceptable PSD (black), restricted by the BGAN spectral mask (dotted red) 18
3.6 Transmitter model used in simulations 19

4.1 The simple spectral mask restricting the sidelobe at $(1+\alpha)/2T$ to be 30 dB below the level of the peak 23
4.2 Transmitted PSD of an ideally predistorted system, restricted by the simple mask close to the mainlobe. 24
4.3 Average transmitted powers for an ideally predistorted system (dotted red) and nonlinear systems, using fixed weight coefficients (black). Transmitted PSD is restricted by the topical mask. 25
4.4 Comparisons of the transmitted PSDs of an ideally predistorted system to different nonlinear systems, all restricted by the topical mask 26
4.5 Average transmitted powers for an ideally predistorted system (dotted red) and nonlinear systems, using various 2-segments weight coefficients (black). Transmitted PSD is restricted by the topical mask. 27
4.6 Average transmitted powers for an ideally predistorted system (dotted red) and nonlinear systems, using various 4-segments weight coefficients (black). Transmitted PSD is restricted by the topical mask. 28

4.7 Average transmitted powers for an ideally predistorted system (dotted red) and nonlinear systems, using various 8-segments weight coefficients (black). Transmitted PSD is restricted by the topical mask. 28
4.8 The simple spectral mask restricting the frequencies larger or equal to $1.7/T$, to be 45 dB below the level of the peak 29
4.9 Transmitted PSD for an ideally predistorted system restricted by the topical spectral mask 30
4.10 Average transmitted powers for an ideally predistorted system (dotted red) and nonlinear systems, using fixed weight coefficients (black). Transmitted PSD is restricted by the topical mask. 31
4.11 Comparisons of the transmitted PSDs of an ideally predistorted system to different nonlinear systems, all restricted by the topical mask 32
4.12 Average transmitted powers for an ideally predistorted system (dotted red) and nonlinear systems, using various 2-segments weight coefficients (black). Transmitted PSD is restricted by the topical mask. 33
4.13 2-segments, B-spline nonlinear characteristic, where $a_1 = 0.485$ 33
4.14 The transmitted PSD, restricted by the topical mask, of an ideally predistorted system (red) and a nonlinear system, with 2-segments where $a_1 = 0.485$. 34
4.15 Average transmitted powers for an ideally predistorted system (dotted red) and nonlinear systems, using various 4-segments weight coefficients (black). Transmitted PSD is restricted by the topical mask. 34
4.16 The transmitted PSDs, restricted by the topical mask, of an ideally predistorted system (red) and a nonlinear system, with 4-segments where $a_1 = 0.58$. 35
4.17 Transmitted PSD of the ideally predistorted system, restricted by the BGAN mask 36
4.18 Average transmitted powers for an ideally predistorted system (dotted red) and nonlinear systems, using fixed weight coefficients (black). Transmitted PSD is restricted by the BGAN spectral mask. 36
4.19 Transmitted PSDs of all considered nonlinear systems with fixed coefficients (black), seen in relation to the BGAN spectral mask (dotted red) 37
4.20 Average transmitted powers for an ideally predistorted system (dotted red) and nonlinear systems, using various 2-segments weight coefficients (black). Transmitted PSD is restricted by the BGAN spectral mask. 37
4.21 Average transmitted powers for an ideally predistorted system (dotted red) and nonlinear systems, using various 4-segments weight coefficients (black). Transmitted PSD is restricted by the BGAN spectral mask. 38

Abbreviations

ACPR	Adjacent Channel Power Ratio
AWGN	Additive White Gaussian Noise
AM/AM	Input-Amplitude-to-Output-Amplitude
AM/PM	Input-Amplitude-to-Output-Phase
BGAN	Broadband Global Area Network
EVM	Error Vector Magnitude
FDMA	Frequency Division Multiple Access
IBO	Input Back-Off
IMD	Intermodulation Distortion
MIMO	Multiple-Input Multiple-Output
PSD	Power Spectral Density
PSK	Phase Shift Keying
QAM	Qadrature Amplitude Modulation
SIR	Signal-to-Interference-Ratio
SNR	Signal-to-Noise-Ratio

Chapter 1

Introduction

1.1 Motivation

Wireless applications have for the last decade experienced an enormous growth, particularly in number of users, but also in range of applications. This increase has not shown any signs to halt in the near future. With this increased usage of the limited resource bandwidth, it is obvious that a service provider with a licence for a specific band wants to exploit this as much as possible. However, the other important resource in telecommunications, transmitted power, will either limit itself with regard to costs, physical limitations of the amplifier and/or interference with neighboring systems in context of bandwidth. Thus, the service provider can not simply increase the transmitted power unlimited. The limitation of costs will not be considered in this thesis.

A power amplifier is limited in such a way that the amplitude characteristic is only linear for low input values. When input values reach, or exceed, a certain level the characteristic of the amplifier becomes nonlinear, and the amplifier will eventually saturate. This nonlinear characteristic causes sidelobes in the transmitted power spectral density (PSD), and may cause interference on adjacent channels. Predistortion is often used to linearize the amplifier and counter the greatest part of the sidelobes. However, if a certain sidelobe level is acceptable, will such a pure linearization scheme be optimal based on transmitted power?

1.2 Objective

The objective of this thesis is finding the optimal resulting nonlinear characteristic for an amplifier using predistortion. With optimal we mean the characteristic that maximizes average transmitted power, while fulfilling given requirements on the out of band spectrum.

1.3 Scope and Limitations

Several simplifications have been made to reduce the complexity, resulting in a sub-optimal approach to find a solution to the problem. We have only examined a specific instance of nonlinearities, namely cubic B-splines, in relevance to a single carrier system. In addition, we have only considered a fraction of all possible B-splines nonlinearities. To reduce the problem even further, these nonlinearities have only been examined in relevance to a small set of various spectral masks. The results obtained should therefore be seen in light of these simplifications, as they do not provide us with an exact solution to the problem. However, the scenarios examined in this thesis span a sufficiently large set of parameters, both with respect to variations in nonlinear characteristic and various spectral masks. Further, if such a nonlinearity exists, we should be able to obtain a coarse estimate of its characteristic.

1.4 Methodology

In this thesis, the problem of sidelobes within the transmitted PSD have been approached in the following matter.

- Restrictions on the transmitted PSD have been placed by means of a spectral mask. This implies that under no cirumstances can the transmitted PSD exceed the PSD of the spectral mask. Depending on the appearance of the mask, we allow for a certain sidelobe level. Hence, we also accept that the cascade of the predistorter and the amplifier may have a somewhat nonlinear characteristic.
- Assumtions that the characteristic of the predistorter and the amplifier is not optimal, as regards average transmitted power from the system as a whole, have been made.
- Examinations of whether or not a nonlinear characteristic that maximizes the average transmitted power from the system as a whole exists have been performed.

Hence, we are dealing with a fairly complex optimization problem, as the optimal nonlinear function is located in the time domain, while our optimization criterion is located in the frequency domain.

1.5 Structure

The rest of this thesis is organized as follows:

Chapter 2 describes important background information which is critical for understanding the work done.

Chapter 3 contains the methodology used and provides an accurate description of the problem and how it has been solved.

Chapter 4 presents the most important results obtained from simulations.

Chapter 5 gives the conclusion of this thesis.

Chapter 2

Background Theory

The main objective of this chapter is to give a thorough introduction to important concepts that are fundamental for understanding the work done and understanding and interpreting the results obtained. A presentation of estimation techniques for the PSD, methods to implement nonlinearities and the impact these have on transmitted signals are included. To fully understand the theory, it is expected that the reader is familiar with fundamental signal processing and advanced calculus.

2.1 Power Spectral Density

The following section gives a basic introduction to the PSD, as well as a more in-depths description of one of several PSD estimation techniques, and is mainly based on [1].

2.1.1 The Periodogram Estimate

The PSD is a measure of how a signal's power is distributed throughout the spectrum. Thus, it is a function of frequency. When $y(t)$ is considered a stationary stochastic process with finite average power, its autocorrelation function is given by

$$\gamma_{yy}(\tau) = E[y^*(t)y(t+\tau)] \tag{2.1.1}$$

where $E[\cdot]$ denotes the statistical average. The PSD of the stationary random process is the Fourier transform of the autocorrelation function

$$\Gamma_{yy}(F) = \int_{-\infty}^{\infty} \gamma_{yy}(\tau)e^{-j2\pi F\tau} \tag{2.1.2}$$

In practice, the true autocorrelation function $\gamma_{yy}(\tau)$ is not known, and as a consequence, we cannot compute $\Gamma_{yy}(F)$. Hence, an estimate of the actual autocorrelation function must be utilized. As for the rest of this section, we assume that a single realization of the random process $y(t)$ is sampled at a rate satisfying the Nyquist sampling theorem, and a finite-duration

sequence $y(n), 0 \leq n \leq N-1$ is obtained. The following estimator is suggested for the autocorrelation function in [1]

$$r_{yy}(m) = \begin{cases} \frac{1}{N} \sum_{n=0}^{N-m-1} y^*(n)y(n+m) & 0 \leq m \leq N-1 \\ \frac{1}{N} \sum_{n=|m|}^{N-1} y^*(n)y(n+m) & m = -1, -2, \ldots 1-N \end{cases} \tag{2.1.3}$$

and it is shown that this is asymptotically unbiased as

$$\lim_{N\to\infty} E[r_{yy}(m)] = \gamma_{yy}(m) \tag{2.1.4}$$

and its variance goes toward zero as $N \to \infty$.

When using the estimator given by (2.1.3), a corresponding estimate of the PSD is given by

$$\begin{aligned} P_{yy}(f) &= \sum_{m=-(N-1)}^{N-1} r_{yy}(m)e^{-j2\pi fm} \\ &= \frac{1}{N}\left|\sum_{n=0}^{N-1} y(n)e^{-j2\pi fn}\right|^2 \\ &= \frac{1}{N}|Y(f)|^2 \end{aligned} \tag{2.1.5}$$

where the second relation comes from inserting (2.1.3) into (2.1.5) and the third relation comes from the definition of the Fourier transform. This relation is called the periodogram. It is further shown [1] that the estimated spectrum, $P_{yy}(f)$, is asymptotically unbiased and that its variance is given by

$$\lim_{N\to\infty} var[P_{yy}(f)] = \Gamma_{yy}^2(f) \tag{2.1.6}$$

as $N \to \infty$. As the variance does not converge to zero, the periodogram is not a consistent estimator of the true PSD.

2.1.2 The Averaged Modified Periodogram

The averaged modified periodogram, or the Welch method, is based on Bartlett's method of averaging periodograms. The Bartlett method works as follows: The N-point input sequence is divided into L non-overlapping segments of length M. For each of these segments, a periodogram is calculated according to (2.1.5). These L segments are then averaged to obtain an estimate of the PSD with smaller variance than the basic periodogram method explained in the previous subsection.

The Welch method is obtained by refining the Bartlett method in two ways [1]. First, the data segments are allowed to overlap, in contrast to the non-overlapping segments of the Bartlett method. In addition, each segment is windowed prior to computation of the periodogram, and this results in the averaged modified periodogram. The mathematical details concerning this

method as well as descriptions of this PSD estimators mean and variance compared to the basic periodogram method can be found in [1]. Due to the scope of this thesis, only the main formulas will be repeated here. The Welch PSD estimate is given by

$$P_{yy}^{W}(f) = \frac{1}{L}\sum_{i=0}^{L-1}\tilde{P}_{yy}^{(i)}(f) \tag{2.1.7}$$

where

$$\tilde{P}_{yy}^{(i)}(f) = \frac{1}{MU}\left|\sum_{n=0}^{M-1} y_i(n)w(n)e^{-j2\pi fn}\right|^2 \quad for \quad i = 0, 1, \ldots, L-1 \tag{2.1.8}$$

is the modified periodogram for each segment and

$$U = \frac{1}{M}\sum_{i=0}^{M-1} w^2(n) \tag{2.1.9}$$

is the normalization factor for the window function $w(n)$.

2.2 Modeling Nonlinearities by Means of B-Splines

A general description of how B-Splines can be utilized as basis functions to produce an estimate of an amplifier characteristic is given in [2], and the main points are repeated below. The relation between an input signal x and an output signal y can be expressed as

$$y(x) = \sum_{j=K_0}^{K-1} a_j B_j(x) \tag{2.2.1}$$

where $B_j(x)$ is the B-spline basis function starting at knot number j, a_j is its corresponding weight coefficient, $K_0 = -3$ when cubic B-splines are used as basis functions and K is equal to the number of intervals in which the input interval is divided into.

When cubic splines are used as basis functions, the $B_0(x)$ function is given as

$$B_0(x) = \begin{cases} \frac{1}{4}\chi^3 & x \in [k_0, k_1\rangle \\ -\frac{3}{4}\chi^3 + \frac{3}{4}\chi^2 + \frac{3}{4}\chi + \frac{1}{4} & x \in [k_1, k_2\rangle \\ \frac{3}{4}\chi^3 - \frac{3}{2}\chi^2 + 1 & x \in [k_2, k_3\rangle \\ -\frac{1}{4}\chi^3 + \frac{3}{4}\chi^2 - \frac{3}{4}\chi + \frac{1}{4} & x \in [k_3, k_4] \end{cases} \tag{2.2.2}$$

The other basis functions can be derived from $B_0(x)$ through the equality

$$B_j(x) = B_0(x - k_j) \tag{2.2.3}$$

The relationship between x and χ is given as

$$k_x = \lfloor K \cdot x \rfloor, \quad \chi = K \cdot x - k_x \tag{2.2.4}$$

where k_x is the interval number in which x is decomposed into.

A common assumption when working with amplifier nonlinearities is utilized by placing the following constraints on the origin

$$y(0) = 0, \quad y''(0) = 0 \tag{2.2.5}$$

These constraints cause the $B_{-3}(x)$ and $B_{-2}(x)$ from (2.2.1) to be zero, and the $B_{-1}(x)$ basis function is modified to

$$B_{-1}(x) = \begin{cases} -\frac{1}{2}\chi^3 + \frac{3}{2}\chi & x \in [k_0, k_1\rangle \\ \frac{3}{4}\chi^3 - \frac{3}{2}\chi^2 + 1 & x \in [k_1, k_2\rangle \\ -\frac{1}{4}\chi^3 + \frac{3}{4}\chi^2 - \frac{3}{4}\chi + \frac{1}{4} & x \in [k_2, k_3\rangle \end{cases} \tag{2.2.6}$$

Figure 2.1 illustrates the basis functions for $K = 6$, and it shows the relationship between the basis functions given by (2.2.3), as well as the appearance of the special $B_{-1}(x)$ function (red).

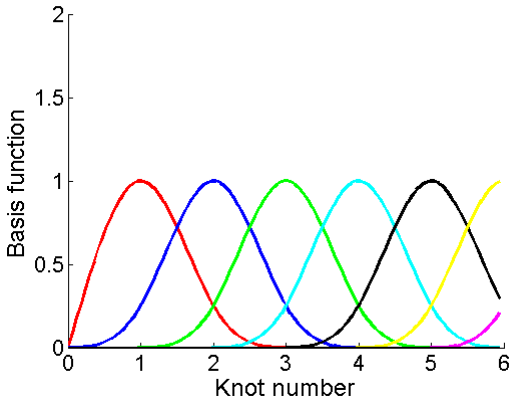

Figure 2.1: B-Spline basis functions when utilizing six segments

A nonlinearity, utilizing K-segments as shown in (2.2.1), provides us with $K + 1$ degrees of freedom when selecting weight coefficients, $\{a_j\}$. As only a fraction of these combinations are interesting in relevance to this thesis, we have placed some limitation on the output-amplitude to input-amplitude (AM/AM) characteristic of y. First, we will consider the set of K-segments nonlinearities where $K + 1$ restrictions are placed on the output signal y. Thereafter we will examine a set of nonlinearities with only K restrictions on the output signal y.

2.2.1 Fixed Weight Coefficients on Nonlinearity

By placing a set of initial conditions on our nonlinearity, we are able to decrease the degrees of freedom. To achieve the desired appearance of our nonlinearity, we first require that the

maximal normalized value of the output signal is obtained when a maximal normalized value is utilized as the input signal. Mathematically, this requirement is given by

$$y(1) = 1, \quad y'(1) = 0 \tag{2.2.7}$$

(2.2.7) decreases the degrees of freedom by two. Thus, to obtain a unique set of weight coefficients $K-1$ additional initial conditions are required. By demanding that the AM/AM characteristic of $y(x)$ is approximately linear up to the last segment, we basically approximate a linear function by means of various K-segments nonlinearities. Mathematically, we demand linear limits between the segments. This results in the following constraints of $y(x)$

$$y''\left(\frac{i}{K}\right) = 0 \quad for \quad i = 1, 2, 3, \ldots, K-1 \tag{2.2.8}$$

Since $y(x)$ depends on the basis functions described by (2.2.2) and (2.2.6), we must derivate these expressions once and twice respectively to be able to represent the first and second derivatives of $y(x)$ used in (2.2.7) and (2.2.8). Thus,

$$B_0'(x) = \begin{cases} \frac{3}{4}\chi^2 & x \in [k_0, k_1\rangle \\ -\frac{9}{4}\chi^2 + \frac{3}{2}\chi + \frac{3}{4} & x \in [k_1, k_2\rangle \\ \frac{9}{4}\chi^2 - 3\chi & x \in [k_2, k_3\rangle \\ -\frac{3}{4}\chi^2 + \frac{3}{2}\chi - \frac{3}{4} & x \in [k_3, k_4] \end{cases} \tag{2.2.9}$$

and

$$B_0''(x) = \begin{cases} \frac{3}{2}\chi & x \in [k_0, k_1\rangle \\ -\frac{9}{2}\chi + \frac{3}{2} & x \in [k_1, k_2\rangle \\ \frac{9}{2}\chi - 3 & x \in [k_2, k_3\rangle \\ -\frac{3}{2}\chi + \frac{3}{2} & x \in [k_3, k_4] \end{cases} \tag{2.2.10}$$

Due to the relation between the basis functions given by (2.2.3), the first and second derivatives of the basis functions $B_i(x)$ for $i = 1, 2, \ldots K-1$ are the same as that of $B_0(x)$ in their appurtenant intervals. As for the first and second derivatives of the basis function, $B_{-1}(x)$, these are

$$B_{-1}'(x) = \begin{cases} -\frac{3}{2}\chi^2 + \frac{3}{2} & x \in [k_0, k_1\rangle \\ \frac{9}{4}\chi^2 - 3\chi & x \in [k_1, k_2\rangle \\ -\frac{3}{4}\chi^2 + \frac{3}{2}\chi - \frac{3}{4} & x \in [k_2, k_3\rangle \end{cases} \tag{2.2.11}$$

and

$$B_{-1}''(x) = \begin{cases} -3\chi^2 & x \in [k_0, k_1\rangle \\ \frac{9}{2}\chi - 3 & x \in [k_1, k_2\rangle \\ -\frac{3}{2}\chi + \frac{3}{2} & x \in [k_2, k_3\rangle \end{cases} \tag{2.2.12}$$

respectively.

The initial conditions stated in (2.2.7), provide us with the following relation between the coefficients that affect the nonlinearity at $y(1)$

$$\begin{aligned} a_{K-3} &= a_{K-1} \\ a_{K-2} &= 1 - \frac{1}{2}a_{K-1} \end{aligned} \tag{2.2.13}$$

The initial conditions given by (2.2.8) were set to approximate a linear function within the first $K-1$ segments. By inserting the second derivatives of the basis functions into (2.2.8) and arranging the resulting expression, we obtain the following relation between the foremost $K-1$ weight coefficients

$$\begin{aligned} a_{-1} &= \frac{1}{2}a_0 \\ a_0 &= \frac{2}{3}a_1 \\ a_1 &= \frac{3}{4}a_2 \\ a_2 &= \frac{4}{5}a_3 \\ &\vdots \\ a_{K-3} &= \frac{K-1}{K}a_{K-2} \end{aligned} \tag{2.2.14}$$

(2.2.14) and (2.2.13) provides us with an equation system with $K+1$ unknown parameters. Combining these by means of linear algebra we obtain the following matrix system

$$\begin{bmatrix} a_{-1} \\ a_0 \\ a_1 \\ \vdots \\ a_{K-3} \\ a_{K-2} \\ a_{K-1} \end{bmatrix} = \begin{bmatrix} 0 & \frac{1}{2} & 0 & \cdots & 0 & 0 & 0 \\ 0 & 0 & \frac{2}{3} & \cdots & 0 & 0 & 0 \\ 0 & 0 & 0 & \cdots & 0 & 0 & 0 \\ \vdots & \vdots & \vdots & \ddots & \vdots & \vdots & \vdots \\ 0 & 0 & 0 & \cdots & 0 & \frac{K-1}{K} & 0 \\ 0 & 0 & 0 & \cdots & 0 & 0 & -\frac{1}{2} \\ 0 & 0 & 0 & \cdots & 1 & 0 & 0 \end{bmatrix} \cdot \begin{bmatrix} a_{-1} \\ a_0 \\ a_1 \\ \vdots \\ a_{K-3} \\ a_{K-2} \\ a_{K-1} \end{bmatrix} + \begin{bmatrix} 0 \\ 0 \\ 0 \\ \vdots \\ 0 \\ 1 \\ 0 \end{bmatrix} \tag{2.2.15}$$

By using vector notation, (2.2.15) can be written as:

$$\begin{aligned} \mathbf{a} &= G\mathbf{a} + \mathbf{b} \\ I\mathbf{a} - G\mathbf{a} &= \mathbf{b} \\ (I-G)\mathbf{a} &= \mathbf{b} \end{aligned} \tag{2.2.16}$$

where I is the identity matrix and the values of $\mathbf{a}$ depend only on K. The unique solution of (2.2.16) can be found using e.g. Matlab. Figure 2.2 illustrates clearly how different nonlinearities can be achieved by means of varying K. It is easy to observe that by increasing K, the resulting nonlinearity becomes increasingly linear, as was our intention with (2.2.8). Thus, as $K \to \infty$ the function becomes linear.

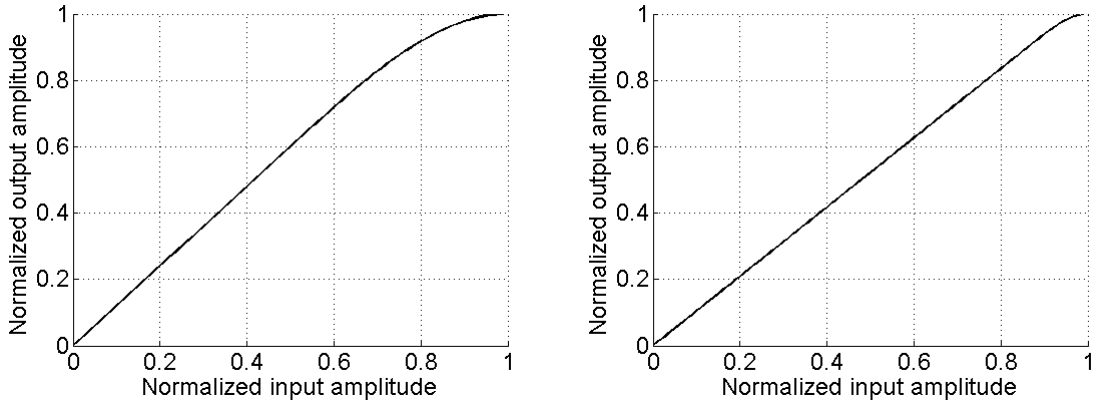

(a) 2-segments nonlinearity

(b) 8-segments nonlinearity

Figure 2.2: Comparison of different nonlinearities using constant weight coefficients

2.2.2 Selecting Weight Coefficients with One Degree of Freedom

The nonlinearity described in the previous subsection with K as the free parameter, is not likely to be the optimal solution of a nonlinearity in relevance to the optimization problem considered in this thesis. However, its complexity is low and it easily provides us with an idea of how many segments that are required in a possible optimal nonlinearity.

A slightly more complex way of implementing the nonlinearity is to allow one degree of freedom in choice of weight coefficients $\{a_j\}$. Basically, the procedure of finding these coefficients are more or less the same as described when using fixed coefficients; We restrict our maximal output value through (2.2.7), but utilize the following restrictions on the double derivatives in place of (2.2.8)

$$y''\left(\frac{i}{K}\right) = 0 \quad for \quad i = 1, 2, 3, \ldots, K-2 \tag{2.2.17}$$

This results in a matrix system with one degree of freedom of coefficients, and it can be expressed as

$$\begin{bmatrix} a_{-1} \\ a_0 \\ a_1 \\ \vdots \\ a_{K-3} \\ a_{K-2} \\ a_{K-1} \end{bmatrix} = \begin{bmatrix} 0 & \frac{1}{2} & 0 & \cdots & 0 & 0 & 0 \\ 0 & 0 & \frac{2}{3} & \cdots & 0 & 0 & 0 \\ 0 & 0 & 0 & \cdots & 0 & 0 & 0 \\ \vdots & \vdots & \vdots & \ddots & \vdots & \vdots & \vdots \\ 0 & 0 & 0 & \cdots & 0 & 0 & 1 \\ 0 & 0 & 0 & \cdots & 0 & 0 & -\frac{1}{2} \\ 0 & 0 & 0 & \cdots & 0 & 0 & 0 \end{bmatrix} \cdot \begin{bmatrix} a_{-1} \\ a_0 \\ a_1 \\ \vdots \\ a_{K-3} \\ a_{K-2} \\ a_{K-1} \end{bmatrix} + \begin{bmatrix} 0 \\ 0 \\ 0 \\ \vdots \\ 0 \\ 1 \\ a_{K-1} \end{bmatrix} \tag{2.2.18}$$

The last coefficient, a_{K-1}, is the free parameter which in principle can be chosen freely. However, there is one limitation: We require that $y(x) \leq 1$ for all values of x.

Because of the mathematical relation between all coefficients $\{a_j\}$ from (2.2.18), we only have to consider the last segment of the nonlinearity, as this segment sets an upper limit of a_{K-1}. The last segment can be derived from (2.2.1) to

$$y(x) = a_{K-4}B_{K-4}(x) + a_{K-3}B_{K-3}(x) + a_{K-2}B_{K-2}(x) + a_{K-1}B_{K-1}(x) \tag{2.2.19}$$

By using the relationship between the coefficients derived in (2.2.18), (2.2.19) can be expressed as

$$y(x) = a_{K-1}\frac{K-2}{K-1}B_{K-4}(x)+a_{K-1}B_{K-3}(x)+(1-\frac{1}{2}a_{K-1})B_{K-2}(x)+a_{K-1}B_{K-1}(x) \quad (2.2.20)$$

where we notice that all addends are related to the unknown weigh coefficient a_{K-1}. Further, by using the definitions of the B-spline basis functions given in (2.2.2),(2.2.3) and (2.2.5), we get

$$\begin{aligned} y(x) = \quad & a_{K-1}(\frac{11}{8}\chi^3 - \frac{15}{8}\chi^2 - \frac{3}{8}\chi + \frac{7}{8}) \\ & +a_{K-1}\frac{K-2}{K-1}(-\frac{1}{4}\chi^3 + \frac{3}{4}\chi^2 - \frac{3}{4}\chi + \frac{1}{4}) \\ & -\frac{3}{4}(\chi^3 - \chi^2 - \chi) + \frac{1}{4} \end{aligned} \quad (2.2.21)$$

By inserting the inequality $y(x) \leq 1$ in (2.2.21) and by moving the last addend that does not contain an a_{K-1} element to the other side of the larger or equal sign we obtain the following inequality.

$$\begin{aligned} \frac{3}{4}(\chi^3 - \chi^2 - \chi + 1) \geq \quad & a_{K-1}\frac{11}{8}(\chi^3 - \frac{15}{11}\chi^2 - \frac{3}{11}\chi + \frac{7}{11}) \\ & -a_{K-1}\frac{1}{4}\frac{(K-2)}{(K-1)}(\chi^3 - 3\chi^2 + 3\chi - 1) \end{aligned} \quad (2.2.22)$$

By means of algebra, the three cubic equations can be solved. As the double root at 1 is equal for all elements, it can be removed, and (2.2.22) is reduced to

$$a_{K-1} \leq \quad \frac{\frac{3}{4}(\chi+1)}{\frac{11}{8}(\chi+\frac{7}{11}) - \frac{1}{4}\frac{(K-2)}{(K-1)}(\chi-1)} \quad (2.2.23)$$

As χ varies from 0 to 1, the right side of (2.2.23) achieves its minimum value for $\chi = 1$. Thus, when we insert this, our demand of $y(x) \leq 1$ gives us the following limitation on the last coefficient

$$a_{K-1} \leq \frac{2}{3} \quad (2.2.24)$$

It should be noted that the maximal value of a_{K-1} is independent of K.

Figure 2.3 demonstrates a set of different nonlinearities that can be obtained by varying the value of a_1 between 0.4 (the most linear curve) and $\frac{2}{3}$ (the curve with the greatest nonlinearity), using 2-segments nonlinearities with one degree of freedom.

2.3 Nonlinear Impact upon a Signal

The impact a random nonlinearity will have on a signal can be observed both in the time domain and the frequency domain. It is custom to separate the nonlinear impact into an AM/AM distortion characteristic and an input-amplitude-to-output-phase (AM/PM) distortion characteristic [3].

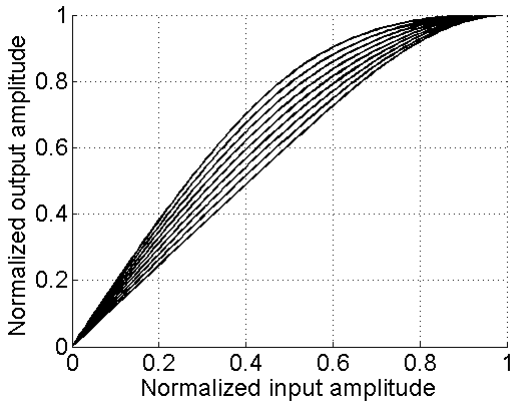

Figure 2.3: Different nonlinearities obtained utilizing a 2-segments nonlinearity, with different accepted values for a_1

2.3.1 Examination of Nonlinear Impact in the Time Domain

The AM/AM distortion can easily be observed in the time domain by means of a scatterplot. Figure 2.4(a) illustrates how the different symbols in a 16-QAM signal are scattered in clusters,

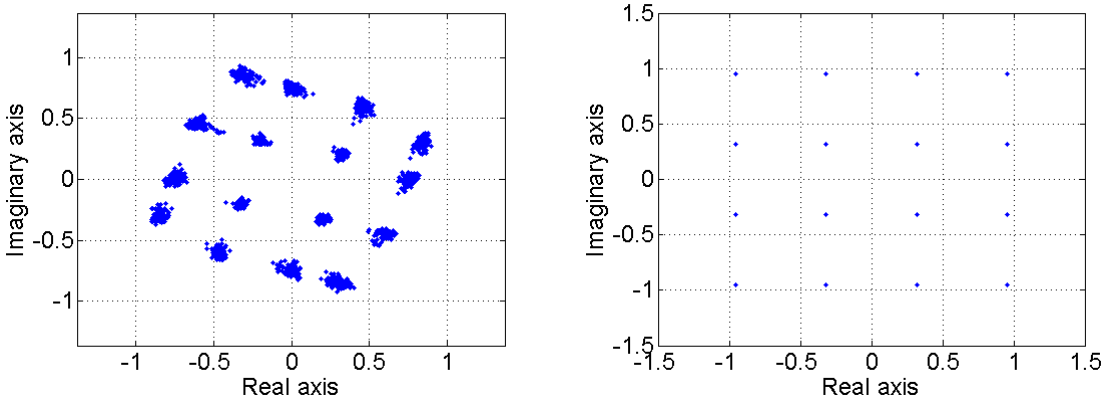

(a) AM/AM and AM/PM distortion

(b) Linear amplification in amplitude and no phase distortion

Figure 2.4: Comparison of a distorted and a nondistorted 16-QAM signal

where they ideally should have been at the same position because of the nonlinear impact.

The AM/PM distortion is also evident here as we notice that the clusters are shifted by the same amount compared to the ideal case in Figure 2.4(b). The AM/PM characteristic is additive and can easily be zeros out with its negative function. However, as it is not of importance in relevance to this thesis we will not examine this any further. Henceforth, we will only consider the AM/AM characteristic when discussing nonlinearities.

2.3.2 Examination of Nonlinear Impact in the Frequency Domain

An important reason for evaluating the transmitted PSD for a specific system, is the fact that these signals can affect adjacent channels [4]. By evaluating the PSD and placing restrictions on our transmitted power outside the mainlobe, we allow adjacent systems to operate as they are supposed to. On the other hand, if this evaluation is not carried out, a worst case scenario is that we may corrupt neighboring systems to such a great extent that they are continuously down.

To understand the impact a nonlinearity have on the PSD, we will consider the general bandpass analog signal

$$x(t) = A(t)\cos(2\pi f_c t + \phi(t) + \theta) \tag{2.3.1}$$

where $A(t)$ is the modulated amplitude as a function of time, f_c is the carrier frequency, $\phi(t)$ is the modulated phase of the signal as a function of time and θ is an arbitrary phase constant. Both $A(t)$ and $\phi(t)$ are distributed in a much lower frequency range than f_c. In this thesis, only the spectrum of $A(t)$ will be considered. The signal $x(t)$ is transmitted through a real-valued and memoryless nonlinearity $g(\cdot)$ which results in the output signal $y(t)$. We will further assume that the nonlinearity $g(x(t))$, and hence $y(t)$, is given by the general equation

$$y(t) = g(x(t)) = b_0 + \sum_{k=1}^{\infty} b_k x^k(t) \tag{2.3.2}$$

Because of the known equality [5]

$$2\cos(nx)\cos(mx) = \cos(n-m)x + \cos(n+m)x \tag{2.3.3}$$

it is clear that the square addend from (2.3.2) will not have frequency elements in the vicinity of $x(t)$

$$\cos^2(2\pi f_c t + \phi(t) + \theta) = \frac{1}{2}(1 + \cos(4\pi f_c t + 2\phi(t) + 2\theta))$$

because $A(t)$ is narrowband compared to f_c, and the frequency elements centered around $2f_c$ can easily be filtered away. When applying (2.3.3) once more, we can prove that the cubic addend from (2.3.2) will have frequency elements in the vicinity of $x(t)$

$$\cos^3(2\pi f_c t + \phi(t) + \theta) = \frac{3}{4}(\cos(2\pi f_c t + \phi(t) + \theta)) + \frac{1}{4}(\cos(6\pi f_c t + 3\phi(t) + 3\theta))$$

and the frequency components centered around $3f_c$ can be filtered away. In fact, if we continue to examine the forth, the fifth etc. addends, we can prove that all even combinations of sinusoids we achieve when inserting (2.3.1) into (2.3.2) will not cause intermodulation distortion (IMD) since f_c is a great many times larger than the bandwidth of $A(t)$. Thus, it can be filtered away.

[6] gives the resulting output from the nonlinearity when the fundamental signal is extracted through trigonometric expansion and a bandpass filter is applied over the wanted frequencies

$$y(t) = \left(b_1 A(t) + \frac{3b_3 A^3(t)}{4} + \frac{5b_5 A^5(t)}{8} + \ldots\right)\cos(2\pi f_c t + \phi(t) + \theta) \tag{2.3.4}$$

As the carrier in (2.3.4) is separate from the rest of the expression, the nonlinear behavior in the first harmonic zone is fully characterised by the expression in the brackets. Multiplication in the time domain corresponds to convolution in the frequency domain [1]. Thus, $A^k(t)$ will correspond to $A(f) * A(f) * ... * A(f)$.

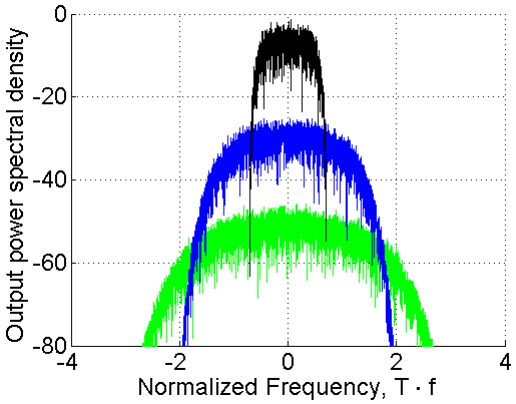

Figure 2.5: PSDs of the linear addend in a baseband signal (black), the cubic nonlinear addend in a baseband signal (blue) and the quintic nonlinear addend in a baseband signal (green)

Figure 2.5 illustrates the different PSDs for a linear addend (black), a cubic addend (blue), and a quintic addend (green), of a 16-QAM modulated signal[1] utilizing a particular set of nonlinearity coefficients, $\{b_k\}$. When these components are added, as given by (2.3.2), we achieve the resultant PSD of the output signal $y(t)$, which is illustrated in Figure 2.6 for the three components considered. When examining the resultant PSD we can easily identify the first and the second sidelobe level caused by the nonlinearity, as well as the mainlobe.

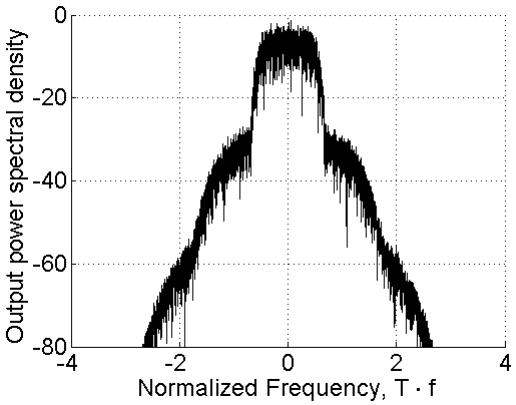

Figure 2.6: The resultant transmitted PSD from a nonlinearity

[1] A cosine rolloff filter with a rolloff factor of 0.4 has been utilized as the transmit filter

Chapter 3

Methodology

This chapter presents the methodology utilized in this thesis. A complete presentation of the problem, and an accurate description of how it has been solved is given. In addition, parameter choices for all simulations are given, as well as fundamental validation and verification of the simulation program implemented.

3.1 System Model

A basic baseband system model based on systems given in [7] which utilizes a nonlinear amplifier and some predistortion scheme to linearize the amplifier, is shown in Figure 3.1. The incoming data bits are modulated into a defined constellation and passed through a transmit filter with impulse response $h(t)$. The resulting time continuous signal is then attenuated by the wanted input back-off (IBO) value before it is predistorted and passed on to the nonlinear amplifier. The signal is then transmitted through a channel with impulse response $c(t)$ and

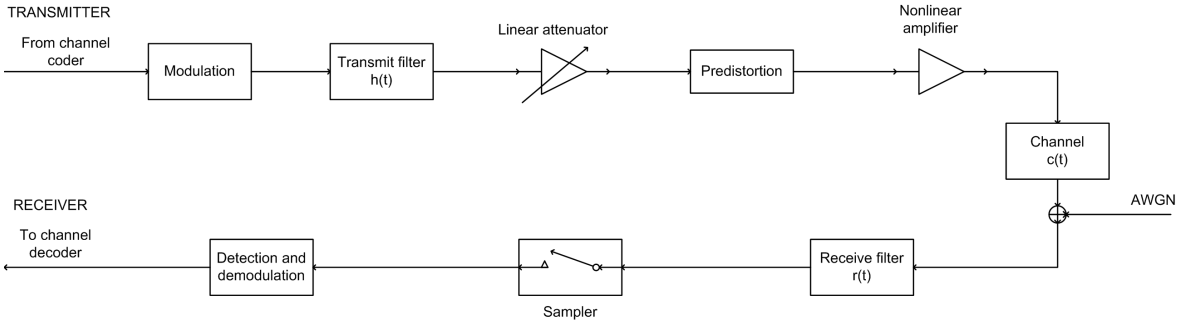

Figure 3.1: A basic baseband system model utilizing a nonlinear amplifier and predistortion

additive white gaussian noise (AWGN) is added to the signal. At the receiver side, the signal goes through the receive filter, gets sampled, and passed on to the demodulator and detector.

The principle of the predistorter is quite simple: A mathematical function that describes the nonlinearity of the amplifier must be found. The incoming signal to the predistorter is then multiplied with the inverse function of the nonlinearity [6]. However, as the true nonlinear

function contains infinite elements, it needs to be estimated, and a wide variety of these estimation methods exists [2, 8, 9, 10]. The thoery is beyond the scope and will not be further discussed.

As the main goal is to maximize the average transmitted power, we will put aside the receiver side of the system model shown in Figure 3.1 and take a closer look on the transmitter side. We assume that the predistorter is capable of equalizing any nonlinearity introduced by the amplifier. The cascade of the predistorter and the amplifier can then be considered an ideal amplification process with a linear AM/AM characteristic up to the saturation point of the amplifier, and with a horizontal AM/AM characteristic afterwards. This assumption is reasonable, as we theoretically can model any nonlinearity as long as we use a sufficiently high order on our estimate of the nonlinear function of the amplifier. For simplicity, we also normalize the signal with regard to average power prior to the linear attenuator.

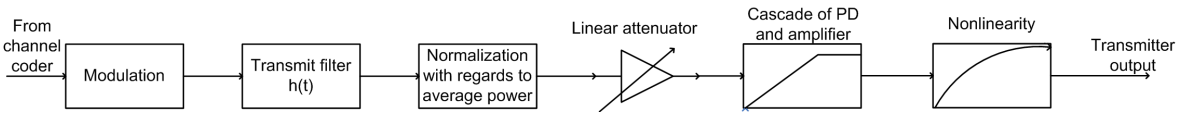

Figure 3.2: The modified transmitter model, where a nonlinear element is inserted, and ideal predistortion is assumed

The main change we do on the transmitter side is adding a nonlinear element subsequent to the cascade. This element will be modeled as various K-segments, B-splines cubic nonlinearities, as explained in Chapter 2.2. The nonlinearity will be modified in each examined scenario by varying the number of segments as well as the degrees of freedom. The resulting transmitter system model is shown in Figure 3.2.

3.2 Optimization Criterion

The main reason for placing restrictions on the transmitted PSD becomes evident in multiuser systems where the spectrum is limited. This is especially important for the wireless channel, but is also of importance for wired multiuser systems. [11] contains a good description of the limitations on the wireless channel, as well as a thorough examination of the frequency division multiple access (FDMA) scheme. [7] describes the general theory of interference experienced on multiple-input multiple-output (MIMO) channels. The essence from these two books, in relation to a shared multiuser channel using the FDMA scheme, boils down to the fact that when we reduce the sidelobe level on the transmitted signal for each user, we reduce the interference between the different transmitted signals. Thus, we increase the probability of detecting the received signals correctly, as the signal-to-interference-ratio (SIR) increases. On the other hand, by reducing the sidelobe level for nonlinear systems we also reduce the total transmitted power on each transmitter. This results in a restriction on how much power each user can transmit at the same time as it reduces the signal-to-noise-ratio (SNR), becuase the noise on the channel do not change independent of how much power is transmitted.

The optimization criterion considered in this thesis, consists of placing certain constraints on the transmitted PSD, henceforth referred to as mask constraints, or simply mask. This mask

can be as simple as requireing the adjacent channel power ratio (ACPR) to be below some threshold for frequencies outside a specific band, or more complex where several thresholds are utilized for different frequencies.

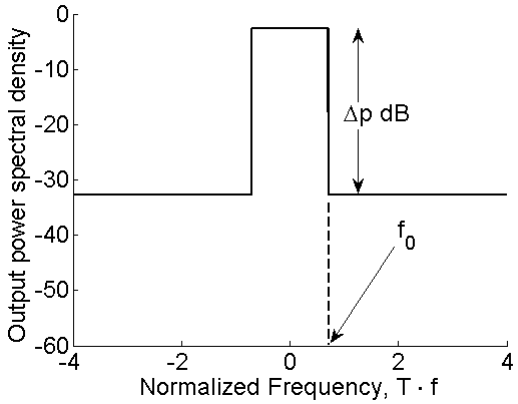

Figure 3.3: Constraining the transmitted PSD with a simple spectral mask

Related to the system model presented in the previous section, our main objective consists of finding the number of, as well as the set of B-spline coefficients $\{a_j\}$ in our nonlinear element that maximize the average transmitted power, but still fulfilling the mask constraints. The first step of finding the optimal $\{a_j\}$ lies in choosing an appropriate mask. In this thesis, we have examined two variations of the simple mask, as well as a more complex mask. The latter is not unlike the one utilized in the broadband global area network (BGAN) [12], henceforth termed the BGAN mask.

The simple mask is illustrated in Figure 3.3 in relation to normalized frequencies, and we can observe that it only depends on a single threshold level, Δp, and a single frequency, f_0, for the baseband system considered. The intention of the mask is quite simple: None of the positive frequencies above or equal to f_0 are allowed to transmit more power/hertz, than given by the difference between the peak and Δp. The same thing applies to the negative frequencies smaller or equal to $-f_0$.

To achieve this reduction, the entire signal needs to be attenuated by an attenuation factor that depends on the number of segments in the nonlinearity utilized, Δp and f_0. On the other hand, as our main objective is maximizing average transmitted power we want to attenuate our signal as little as possible.

We will now turn our focus from the simple mask to the BGAN mask. Figure 3.4 illustrates the BGAN mask in relation to normalized frequencies. We note that in contrast to the simple mask that only have two levels, the BGAN mask have threshold levels based on four different frequencies. The intention of this mask is the same as for the simple mask. We place the BGAN mask on top of the transmitted spectrum with the peak of the mask at the same level as that of the peak of the PSD. The transmitted PSD is found acceptable if its power density lies below the mask for all frequencies. Else, more attenuation is required to fulfill the mask. Figure 3.5 shows a comparison of such an acceptable PSD (a) and a non-acceptable PSD (b) restricted by the BGAN spectral mask. It is easy to observe that the PSD exceeds the mask in the latter case.

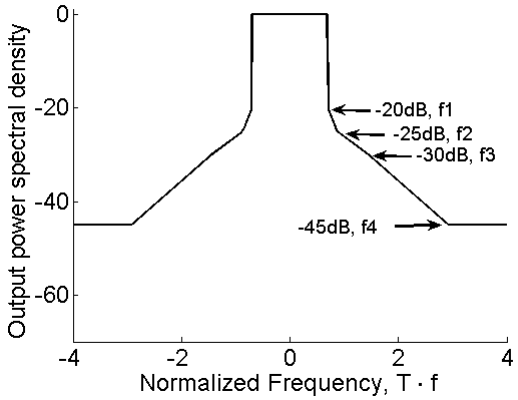

Figure 3.4: Constraining the transmitted PSD with the BGAN spectral mask

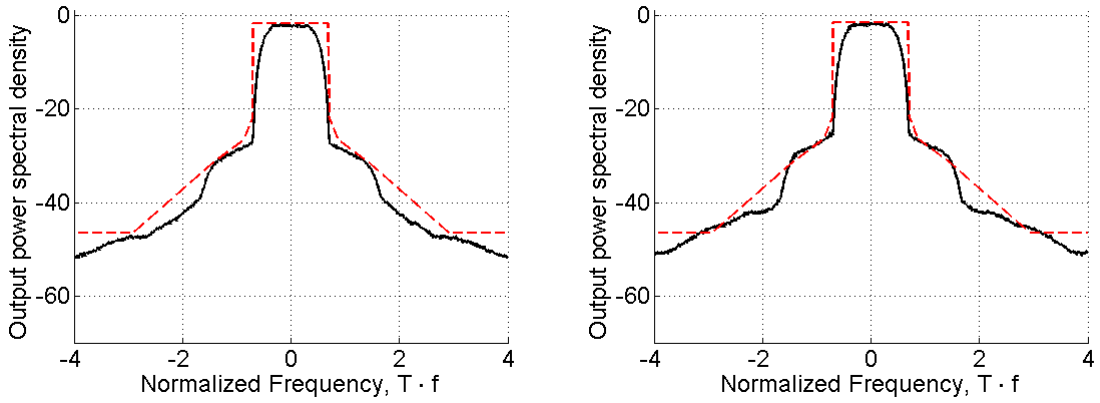

(a) Acceptable PSD

(b) Non-acceptable PSD

Figure 3.5: Comparison of an acceptable and a non-acceptable PSD (black), restricted by the BGAN spectral mask (dotted red)

The optimization problem utilized in this thesis can now be formalized. Given a spectral mask and a system model as the one described in Chapter 3.1; by varying the number of segments and degrees of freedom in the nonlinear element we want to do the following: For each nonlinear variation, find the minimum attenuation factor needed to keep the PSD below the spectral mask. Then calculate the average transmitted power of such a system, and compare this result to the average transmitted power of an ideally predistorted system restricted by the same mask.

3.3 Simulation Environment

All simulations in this thesis have been performed using Matlab version 7.4.0.287 with the Signal Processing Toolbox installed. Some of the basic operations in relation to the system model described in Chapter 3.1 are executed by *.m files written and/or revised by Frank

Lotku and/or Nils Holte. These functions have been assumed to function correctly, and have thus been omitted when validating and verifying the simulation program.

3.4 Simulations - A Statistical Approach

The system model presented in Chapter 3.1 is continuous-time. Thus it is not implementable when utilizing the discrete-time simulation environment Matlab. Hence, to be able to implement it the transmitter model shown in Figure 3.2 requires modifications. In addition, parameters like modulation scheme and transmit filter have to be chosen.

System Parameter	*Value*
Modulation Scheme	16-QAM
Transmit Filter	Square Root Cosine Rolloff Filter
Rolloff Factor, α	0.4
Oversampling rate, T	8
Number of symbols, K	4096
Number of runs for averaging samples, N	50

Table 3.1: Simulation parameters

Table 3.1 summarizes these design choices, while Figure 3.6 illustrates the transmitter model after it is discretizated and modified with the listed choices. The choice of 16-QAM as our

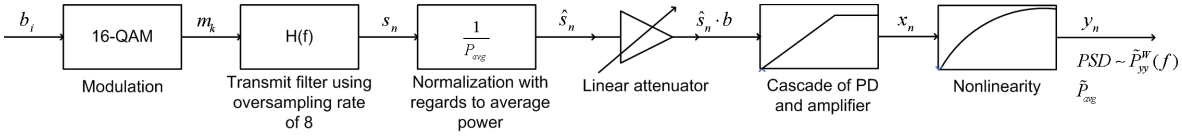

Figure 3.6: Transmitter model used in simulations

modulation scheme was somewhat accidental, and several other modulation schemes could easily have been utilized in its place. However, the modulation scheme is not a crucial parameter in context to the problem adressed in this thesis, so 16-QAM has remained our choice for simplicity. The number of symbols to be transmitted, K, is on the other hand a more important parameter, as it has a direct influence on the quality of our estimated variables. As for the transmit filter, this was chosen as a cosine rolloff filter to satisfy Nyquist criterion [7]. The choice of rolloff factor was suggested by STM Norway, and an oversampling rate, T, of 8 was chosen.

We consider a complete run of all symbols through the system a single realization of a stationary stochastic process [13]. Thus, each single sample y_n can also be considered a stochastic process, with an expectation value equal to zero and a variance equal to the true average transmitted power, P_{avg}. A signal of length $K \times T$ that passes through the system will therefore result in the average transmitted power estimate $\tilde{P}_{avg}$ through

$$\tilde{P}_{avg} = \frac{1}{K \cdot T} \sum_{n=0}^{K \cdot T - 1} |y_n|^2 \tag{3.4.1}$$

and a PSD estimate $\tilde{P}_{yy}^{W}(f)$, where $\tilde{P}_{yy}^{W}(f)$ is calculated by means of the averaged modified periodogram described in Chapter 2.1.2, using the parameters listed in Table 3.2.

The averaged modified periodogram	
w(n)	Hamming window
Window Length, M	1024
Number of segments, L	31
Overlap	50 %

Table 3.2: Parameters used when estimating the transmitted PSD in relevance to (2.1.7)-(2.1.9)

By means of estimation theory [14], we can improve our current estimates of average transmitted power and PSD. As we consider a complete run through the system a single realization of a stationary stochastic process, we also consider $\tilde{P}_{avg}$ and $\tilde{P}_{yy}^{W}(f)$ to be samples from that single experiment. Thus, by performing N runs, we obtain N samples, which can be applied to improve our initial estimates. With that, our new estimate for average transmitted power becomes

$$\bar{P}_{avg} = \frac{1}{N}\sum_{i=0}^{N-1} \tilde{P}_{avg}^{(i)} \tag{3.4.2}$$

and the formula for our new estimate of the PSD will be the same as (3.4.2) where P_{avg} is replaced with $P_{yy}^{W}(f)$. The variance for each sample can be found through the sample-variance estimation function

$$\tilde{S}_{Pavg}^{2} = \frac{1}{N-1}\sum_{i=0}^{N-1} (\tilde{P}_{avg}^{(i)} - \bar{P}_{avg})^2 \tag{3.4.3}$$

Finally, the standard deviation for the estimate $\bar{P}_{avg}$ can be found through

$$\bar{S}_{Pavg} = \frac{\tilde{S}_{Pavg}}{\sqrt{N}} \tag{3.4.4}$$

As both mean and variance are estimated quantities, a T-distribution must be utilized. However, [14] states that if the sample size is large enough ($N \geq 30$), the distribution of T does not differ considerably from the standard normal distribution and we can conclude that

$$P(\bar{P}_{avg} - 3 \cdot \bar{S}_{Pavg} \leq P_{avg} \leq \bar{P}_{avg} + 3 \cdot \bar{S}_{Pavg}) \approx 99\% \tag{3.4.5}$$

As stated in Table 3.1, N has been set to 50 for all simulations preformed in this thesis.

3.5 Confirmation of Simulation Program

Validation describes whether some software satisfies its intended use and whether the results obtained from the simulations are sufficiently accurate, while verification describes whether the software is implemented correctly [15].

Validation

A computer program capable of simulating the system model illustrated in Figure 3.6 has been implemented using the parameters enlisted in Table 3.1. The implementations have been done in such a way that it is possible to utilize one of the following options for the nonlinear element in system

- A linearity, resulting in what we henceforth will refer to as an ideally predistorted system
- A K-segments B-spline nonlinearity with fixed spline coefficients where K is the free parameter. A theoretical description of this nonlinearity is given in Chapter 2.2.1
- A K-segments B-spline nonlinearity with one degree of freedom in choice of spline coefficients, but where K is set constant. A description of this is given in Chapter 2.2.2

Subsequent to the nonlinear element, estimates of the PSD and the average transmitted power are computed as described in Chapter 3.4. To further improve these estimates, we have embedded the program within a loop counting from 1 to 50, so averaging a set of 50 initial estimates for the PSD and the average transmitted power, gives the final estimates.

The final estimate of the PSD is seen in relation to one of the different spectral masks, described in Chapter 3.2. If the requirements placed by the mask are fulfilled, the final estimate of the average transmitted power is stored, and later used to compare against other similar estimates. Else, we increase the attenuation factor, and redo the experiment.

As described above, the implemented simulation program is capable of solving the sub-optimal optimization problem addressed in this thesis. It also produces quite accurate estimates of both the PSD and the average transmitted power, as our intention was by averaging 50 samples. Thus, we conclude that the implemented software satisfies its intention as well as producing sufficiently accurate results.

Verification

Verification of the implemented simulation program has been preformed using so-called black box testing, where each element illustrated in Figure 3.6 has been tested based on known input versus expected and measured output values. Additionaly, the estimates of the PSDs have been examined visually in relevance to restrictions placed by different spectral masks. As mentioned in Chapter 3.3, some of the building blocks have been assumed to function correctly. These include generation of the modulated signals $\{m_k\}$ and filtering through the cosine rolloff filter. Thus, the symbol sequence of all $\{s_n\}$ will form the basis in the following unit tests.

Normalization with regard to average power has been tested by insuring that the sequence of all $\{\hat{s}_n\}$ have an average power equal to 1, and the attenuation operation has simply been done by multiplying the sequence $\{s_n\}$ with b. To verify the exactness of the cascade element we have measured the maximal amplitude subsequent to this element and ensured that none of the different $\{x_n\}$ have amplitude values higher than 1.

The nonlinear element has been tested independent of the rest of the system. This test has been performed for a set of different fixed K-segments nonlinearities by varying K, as well

as a set of different K-segments nonlinearities with one degree of freedom[1]. The test has been performed transmitting a known input vector $\mathbf{x}$ of length 1000, where $x_n = n/1000$, through the nonlinear element. The output vector, $\mathbf{y}$, has been plotted, and the maximum and minimum values have been calculated. The following conditions have been used as a basis to verify the correctness of the nonlinear element

- $y(0) = 0$
- $y(1) = 1$
- $y(x) \leq 1$ for $x \leq 1$
- $\mathbf{y}$ is more linear for large K than for small K
- Utilization of an a_{K-1} weight coefficient larger than $2/3$ results in an invalid nonlinearity

All test performed indicate that the correctness of the implementation is sufficient. However, should the program contain bugs, these have not proved to be of any importance to the results considered in this thesis.

[1] Variaton in both K and the free parameter a_{K-1}

Chapter 4

Simulation Results

In this chapter we will present results obtained based on different simulation scenarios. All results have been obtained utilizing the system model illustrated in Figure 3.6 by examining different nonlinearities.

The main results presented here are average transmitted powers for the different nonlinear systems compared to similar linear system restricted by the same spectral mask.

4.1 A Simple Mask close to the Mainlobe

The first set of simulations were done utilizing a simple mask, as the one illustrated in Figure 4.1, where the value for Δp was set to 30 dB and the frequency point at f_0 was set to $(1+\alpha)/2T$.

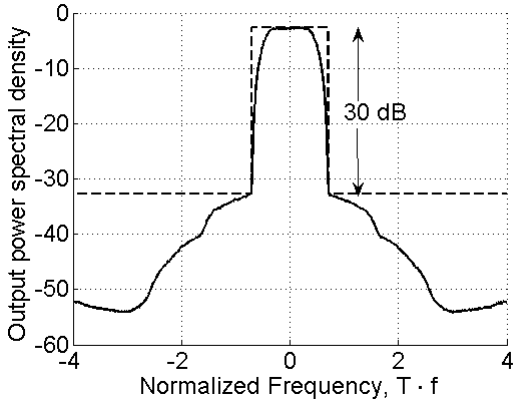

Figure 4.1: The simple spectral mask restricting the sidelobe at $(1+\alpha)/2T$ to be 30 dB below the level of the peak

However, to make the implementation more resistant to statistical variations in the PSD, the peak value was calculated by averaging all values of the PSD estimate for

$$\frac{1-\alpha}{2T} \leq f \leq \frac{1-\alpha}{2T} \tag{4.1.1}$$

The same thing was also done when we calculated the dB value at f_0, but here we only considered the positive side of the PSD estimate

$$\frac{1+\alpha}{2T} \cdot 1.0025 \leq f \leq \frac{1+\alpha}{2T} \cdot 1.015 \tag{4.1.2}$$

As for the choice of coefficients 1.0025 and 1.015, these were chosen on an empirical basis from visual examination of the PSD estimate, as they proved to give a fairly good estimate of the actual break of the curve just outside the mainlobe.

4.1.1 An Ideally Predistorted System

In order to find out whether a nonlinear system outperforms an ideally predistorted system, based on average transmitted power, we will first examine the results obtained from an ideally predistorted system, restricted by the spectral mask as described above. By utilizing the statistical methods as described in Chapter 3.4, we obtain an estimate of the transmitted PSD, which is illustrated in Figure 4.2, and Table 4.1 summarizes the most important results

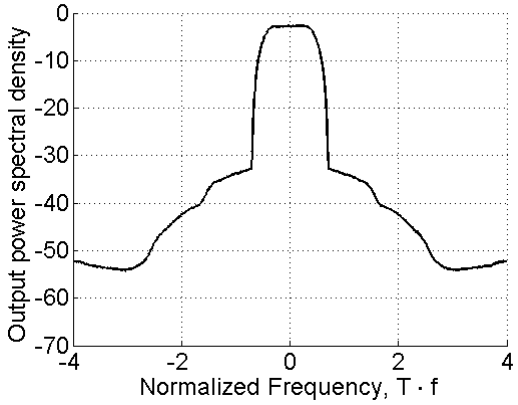

Figure 4.2: Transmitted PSD of an ideally predistorted system, restricted by the simple mask close to the mainlobe.

achieved. When considered alone, these results do not provide us with any relevant information apart from the fact that the estimator, $\bar{P}_{avg}$, has a very small variance, and is thus a good estimate of the actual transmitted power. However, when compared against results obtained from similar nonlinear systems, it should become clear whether or not a certain nonlinear system is capable of outperforming an ideally predistorted system.

Measured variable	*Estimated Value*
Average transmitted power, $\bar{P}_{avg}$	0.5184 [Normalized]
Standard deviation, $\bar{S}_{Pavg}$	0.0002 [Normalized]
IBO, linear/dB	0.74 [Linear]/-1.3077 [dB]

Table 4.1: Estimated parameters for the ideally predistorted system

4.1.2 Nonlinear Systems

The analysis concerning different nonlinear systems will be presented as follows: First, we will examine a set of nonlinear systems with zero degrees of freedom, as explained in Chapter 2.2.1. Secondly, we will examine selected nonlinear systems with one degree of freedom in weight coefficients, as explained in Chapter 2.2.2.

Fixed Weight Coefficients

When using fixed weight coefficients we approximate a linear curve with a K-segments nonlinearity. Hence, by increasing the number of coefficients, K, we are approximating a linearity. Because of this, we are not particularly interested in examining nonlinearities for large K, and have limited our set of nonlinearities to $2 \leq K \leq 10$. For each of these, we have calculated estimates of the average transmitted power, based on the topical spectral mask. Figure 4.3

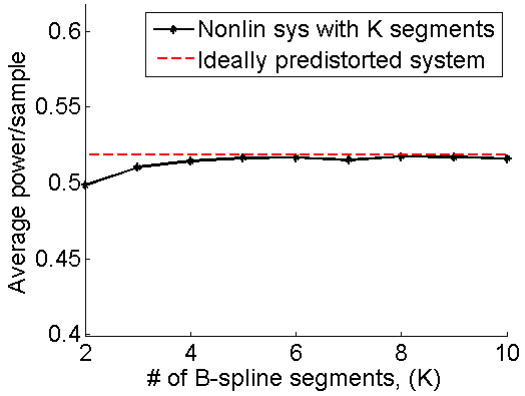

Figure 4.3: Average transmitted powers for an ideally predistorted system (dotted red) and nonlinear systems, using fixed weight coefficients (black). Transmitted PSD is restricted by the topical mask.

illustrates the average transmitted powers[1] for these nonlinearities, compared to the ideally predistorted case. By examining the plot, we can easily observe that none of these particular nonlinear systems achieves an average transmitted power as high as that of an ideally predistorted system. In fact, the average transmitted powers for the lowest K are clearly weaker, and in the worst case for $K = 2$ it is only 96.1 % of the average transmitted power of an ideally predistorted system. As for the other end of the scale, when we increase K, we can observe that the average transmitted power of such a system goes toward the result obtained for an equvialent ideally predistorted system, which is as expected. Already at five segments, we achieve a transmitted power of approximately 99.5 % of the idelly predistorted system, and this is kept more or less constant up to the maximum value of K which has been considered in this thesis. However, we can observe from Table 4.2 that the lower K require more IBO to keep their PSDs below the spectral mask.

[1]The average transmitted powers are estimated values and have all small standard deviations($\bar{S}_{Pavg} \leq 0.0002$)

Number of segments (K)	$\bar{P}^{\%}_{avg}$ *of linear system*	IBO [linear]/[dB]
2	96.1 %	0.615/-2.1112
3	98.5 %	0.657/-1.8243
4	99.2 %	0.678/-1.6877
5	99.6 %	0.691/-1.6052
6	99.7 %	0.699/-1.5552
7	99.4 %	0.703/-1.5304
8	99.8 %	0.709/-1.4935
9	99.7 %	0.712/-1.4752
10	99.6 %	0.714/-1.4630

Table 4.2: Estimated parameters for different nonlinear systems using fixed coefficients.

Figure 4.4 illustrates the transmitted PSD of a system utilizing a 2-segments nonlinearity (a) and the transmitted PSD of a system utilizing an 8-segments nonlinearity (b), both compared to the transmitted PSD of an ideally predistorted system. The PSD of the 2-segments nonlinearity stands clearly out from the other two, as the sidelobe level in the vicinity of ± 2, is distinctly lower than both the ideally predistorted and the 8-segments nonlinearity.

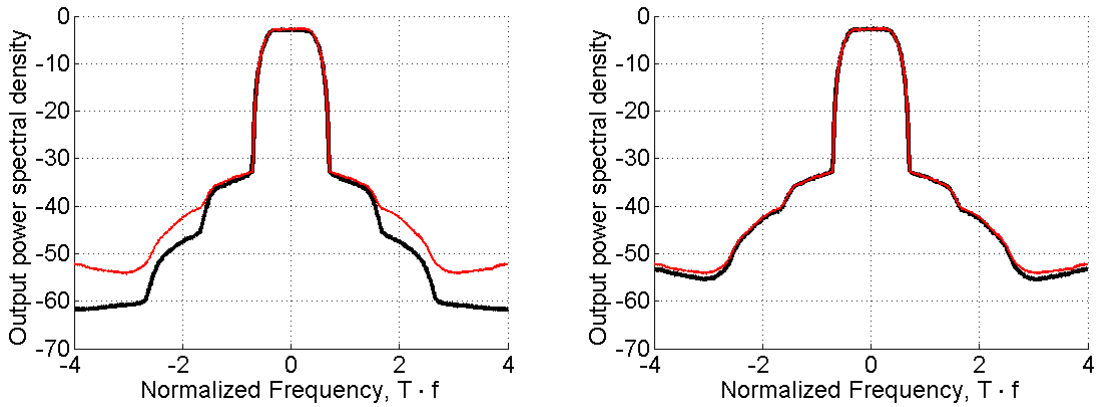

(a) Nonlinear system with 2-segments (black) and an ideally predistorted system (red)

(b) Nonlinear system with 8-segments (black) and an ideally predistorted system (red)

Figure 4.4: Comparisons of the transmitted PSDs of an ideally predistorted system to different nonlinear systems, all restricted by the topical mask

Two Segments Nonlinearity with One Degree of Freedom

The nonlinear system that utilizes a 2-segments nonlinearity with fixed coefficients, does not produce a more power efficient scheme than an ideally predistorted system. However, we are able to create notable different nonlinearities for a 2-segments nonlinearity by varying the weight coefficient a_1, as was illustrated in Figure 2.3. We performed a set of 72 new experiments, where the a_1 weight coefficient was varied between 0.3 and 0.66. For each of these different nonlinear systems, we calculated estimates of the transmitted PSD and the

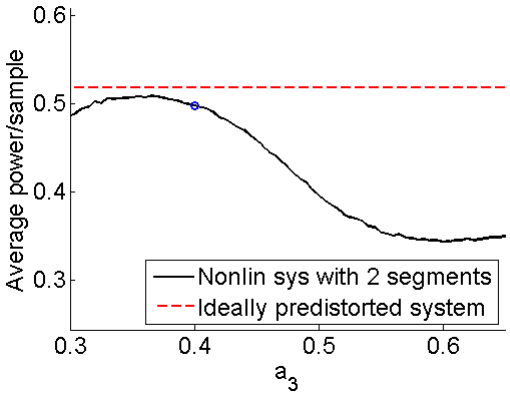

Figure 4.5: Average transmitted powers for an ideally predistorted system (dotted red) and nonlinear systems, using various 2-segments weight coefficients (black). Transmitted PSD is restricted by the topical mask.

average transmitted power. Figure 4.5 illustrates the average transmitted powers of these nonlinear systems (solid black), compared to the ideally predistorted system (dotted red). The blue circle illustrates the average transmitted power for a system utilizing a 2-segments nonlinearity with fixed coefficients.

We can easily observe that a maximum is achieved when a specific weight coefficient is utilized in the nonlinear element of the system, and we can further notice that this weight coefficient is slightly lower than the one marked with the blue circle. However, none of these nonlinear systems are capable of increasing the average transmitted power that is achieved by an ideally predistorted system. In fact, the best 2-segments nonlinearity, ($a_1 = 0.365$), is only capable of transmitting approximately 98 % of the average power achieved by an ideally predistorted system, while the largest a_1 values, only provide us with average transmitted powers as poor as 66 % compared to an ideally predistorted system. It should also be mentioned that all considered systems, utilizing 2-segments nonlinearities, require noticably more IBO attenuation than an ideally predistorted system, to meet the requirements set by the topical spectral mask.

By examining Figure 4.5, we can conclude that none of the systems, utilizing 2-segments nonlinearities, are capable of outperforming an ideally predistorted system.

Four Segments Nonlinearity with One Degree of Freedom

We observed that when using fixed coefficients, the system utilizing a 4-segments nonlinearity obtained higher average transmitted power than the one using 2-segments. Hence, we will take a closer look at systems utilizing different 4-segments nonlinearities and allow one degree of freedom at the last weight coefficient. Figure 4.6 illustrates the average transmitted power for systems utilizing these nonlinearities (solid black), compared to the ideally predistorted system (dotted red). We can observe that the weight coefficient in the nonlinearity that offers the highest average transmitted power, also for 4-segments, lies a few hundreds below the coefficient used in the fixed case (blue circle).

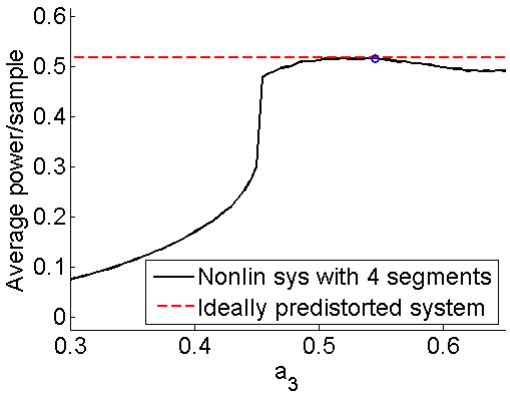

Figure 4.6: Average transmitted powers for an ideally predistorted system (dotted red) and nonlinear systems, using various 4-segments weight coefficients (black). Transmitted PSD is restricted by the topical mask.

Nevertheless, none of the systems utilizing 4-segments nonlinearities achieve higher average transmitted power than an ideally predistorted system. The best result we obtain, is an average transmitted power of approximately 99.7 % of the ideally predistorted system when using the weight coefficient $a_3 = 0.52$.

Eight Segments Nonlinearity with One Degree of Freedom

Figure 4.7 illustrates the results obtained by considering systems utilizing various 8-segments nonlinearities. By setting the a_7 value a few hundreds below the one used in the fixed nonlinearity, we obtain a power efficiency that is approximately equal to that of an ideally predistorted system, but neither for these cases will any of the nonlinear systems outperform an ideally predistorted system.

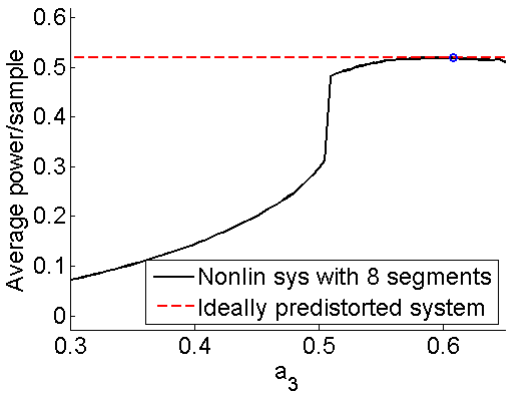

Figure 4.7: Average transmitted powers for an ideally predistorted system (dotted red) and nonlinear systems, using various 8-segments weight coefficients (black). Transmitted PSD is restricted by the topical mask.

4.1.3 Important Observations

This section has dealt with spectral restrictions placed on a sidelobe level close to the mainlobe, with a Δp value equal to 30 dB. Simulations with Δp values equal to 20 dB and 40 dB have also been executed, but these results are omitted here as they only support that an ideally predistorted system is the optimal solution when restrictions are placed close to the mainlobe.

4.2 A Simple Mask at 1.7/T

In the previous section we showed that none of the nonlinear systems considered in this thesis were able to outperform an ideally predistorted system, based on average transmitted power when placing restrictions close to the mainlobe. In this section we will consider a slightly different scenario: By allowing unlimited power density within the first sidelobe level, we want to examine whether this affects the proportions in average transmitted powers between the ideally predistorted system and various nonlinear systems. Figure 4.8 illustrates the spectral mask used in these scenarios. The value of Δp was set to 45 dB, while f_0 was set to $(3+\alpha)/2T$, which corresponds to $1.7/T$ as a rolloff factor of 0.4 was used.

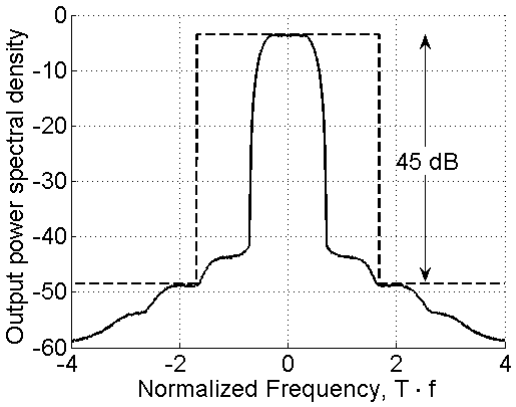

Figure 4.8: The simple spectral mask restricting the frequencies larger or equal to $1.7/T$, to be 45 dB below the level of the peak

The peak in the estimated PSD was calculated through (4.1.1), and a statistical approach was also used here to find a fairly good estimate of the power density at $1.7/T$ by averaging the power densities for the following frequency values

$$\frac{3+\alpha}{2T} \cdot 0.993 \leq f \leq \frac{3+\alpha}{2T} \cdot 1.0055 \tag{4.2.1}$$

4.2.1 An Ideally Predistorted System

Figure 4.9 illustrates the estimated PSD of a signal that passes through an ideally predistorted system restricted by the topical spectral mask.

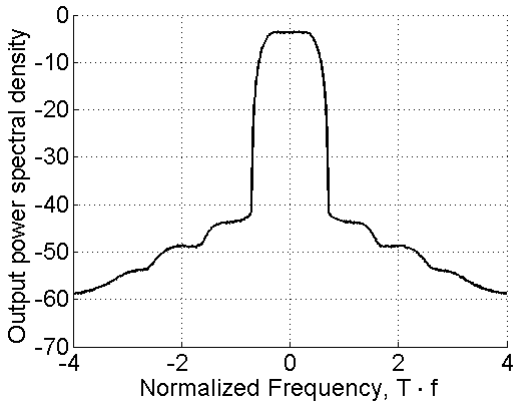

Figure 4.9: Transmitted PSD for an ideally predistorted system restricted by the topical spectral mask

We note that the PSD has a very dominant peak, and that the first sidelobe level is located almost as low as the second sidelobe level. Thus, by placing a mask at $1.7/T$ for an ideally predistorted system we also obtain a low sidelobe level for the first sidelobe, which was considered in the previous section. Table 4.3 summarizes the most important estimated parameters obtained from simulating the described ideally predistorted system. We notice that the average

Measured variable	*Estimated Value*
Average transmitted power, $\bar{P}_{avg}$	0.4254 [Normalized]
Standard deviation, $\bar{S}_{Pavg}$	0.0001 [Normalized]
IBO, linear/dB	0.656 [Linear]/-1.8310 [dB]

Table 4.3: Estimated parameters for an ideally predistorted system

transmitted power is noticeable lower compared to the ideally predistorted system considered in the previous section (Table 4.1). However, this is an expected result as more attenuation is needed to fulfill the spectral mask. This can also be observed in the two spectra, where the entire PSD in Figure 4.9 basically lies lower than the one shown in Figure 4.2.

4.2.2 Nonlinear Systems

This presentation of different nonlinear systems restricted by the topical spectral mask, will follow an outline resembling the one in the previous section.

Fixed Coefficients in Nonlinearities

Figure 4.10 illustrates the average transmitted powers for nine various nonlinear systems, utilizing different K in their respective nonlinear elements (black), compared to the average transmitted power of an ideally predistorted system (dotted red). What we immediately notice, is that average transmitted power as function of number of segments is the opposite of the one illustrated in Figure 4.3. By only placing spectral restrictions in the vicinity of the

second sidelobe level, it is quite obvious from Figure 4.10 that a system utilizing a 2-segments nonlinear element with fixed weight coefficients, will outperform an ideally predistorted system, as regards average transmitted power, with approximately 3 %. In addition, we can observe that the nonlinear systems utilizing large K with fixed coefficients, also with this spectral restriction will produce approximately the same average transmitted power as an ideally predistorted system.

Figure 4.11 illustrates the transmitted PSD of a signal passing through a system utilizing a fixed 2-segments nonlinearity (a) and an fixed 8-segments nonlinearity (b), both compared to the PSD of an ideally predistorted system. While the transmitted PSDs for the ideally predistorted system and the 8-segments nonlinear system are more or less equal, the system utilizing a 2-segments fixed nonlinearity stands out as the transmitted power in the first sidelobe is several decibel higher than that for an ideally predistorted system.

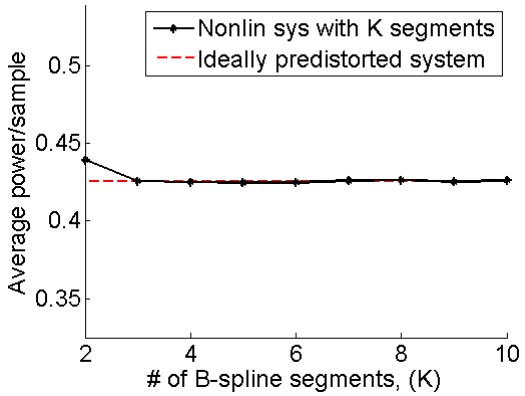

Figure 4.10: Average transmitted powers for an ideally predistorted system (dotted red) and nonlinear systems, using fixed weight coefficients (black). Transmitted PSD is restricted by the topical mask.

Two Segments Nonlinearity with One Degree of Freedom

As we observed, a transmitter utilizing a 2-segments B-spline nonlinear element with fixed coefficients is able to slightly increase the average transmitted power obtained by an ideally predistorted system. As this is probably not the optimal nonlinearity with respect to the highest possible average transmitted power, we have examined whether another value of a_1 for a 2-segments nonlinearity can perform even better. A total of 72 different values of a_1, ranging from 0.3 to 0.66, have been considered, and estimates of their average transmitted powers been calculated for each scenario. Figure 4.12 illustrates these as a function of the weight coefficient a_1 (solid black) as well as the average transmitted power estimate for an ideally predistorted system (dotted red). The blue circle represents the transmitted power when utilizing a fixed 2-segments nonlinearity.

What we immediately observe from the figure, is the tremendous increase in average transmitted power, in fact as much as 52 % compared to an ideally predistorted system. As this is clearly a peak on a quite smooth curve, it seems that the nonlinearity as illustrated in

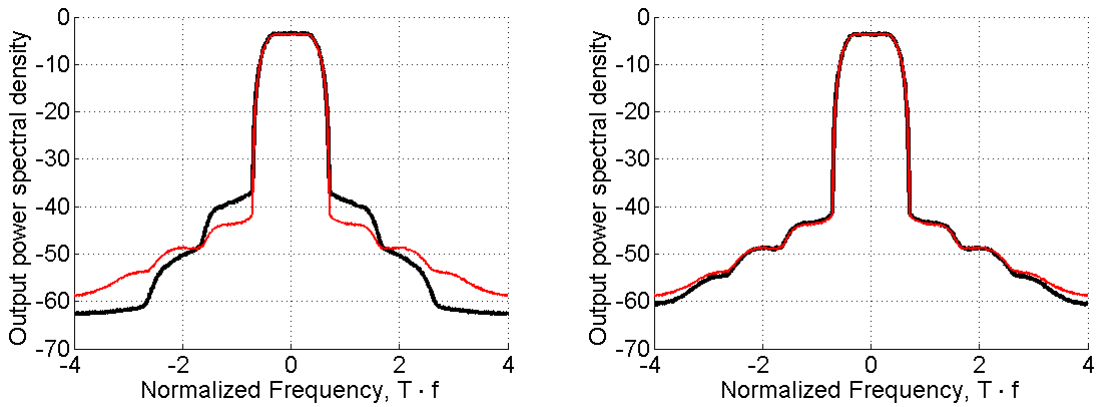

(a) Nonlinear system with 2-segments (black) and an ideally predistorted system (red)

(b) Nonlinear system with 8-segments (black) and an ideally predistorted system (red)

Figure 4.11: Comparisons of the transmitted PSDs of an ideally predistorted system to different nonlinear systems, all restricted by the topical mask

Figure 4.13 utilizing an a_1 coeffecient equal to 0.485 is optimal. However, as the difference in transmitted power is so pronounced we also want to examine its transmitted PSD, which is illustrated in Figure 4.14 (black) compared to the ideally predistorted system (red). We can easily observe that the two spectra differ by a huge amount. While the PSD of the nonlinear system has a difference between its peak and its first sidelobe of approximately 20 dB, the same difference for the PSD of the ideally predistorted system is almost 40 dB.

Four Segments Nonlinearity with One Degree of Freedom

We have also examined a set of different systems utilizing 4-segments nonlinearities with one degree of freedom, in the same way as was done with 2-segments, and the results in average transmitted power can be seen in Figure 4.15. When comparing these results to the highest average transmitted power obtained from the 2-segments nonlinearities, it becomes obvious that none of the systems utilizing 4-segments nonlinearities are capable of coming close to the great increase of 52 %. However, this nonlinearity is capable of increasing the transmitted power by a small amount (4.1 % increase) when utilizing 0.58 as the a_3 coefficient, and we can observe from Figure 4.16 that the PSD of this system has a difference of approximately 35 dB between its peak and its first sidelobe level.

4.2.3 Important Observations

The results presented here clearly shows that an ideally predistorted system is not the optimal solution with respect to average transmitted power when a simple spectral mask at $1.7/T$ is utilized. The nonlinearities that achieves 50 % more transmitted power have tremendous higher sidelobe level at the first sidelobe, and will probably not be desireable even though they outperform the ideally predistorted system to such a great extent.

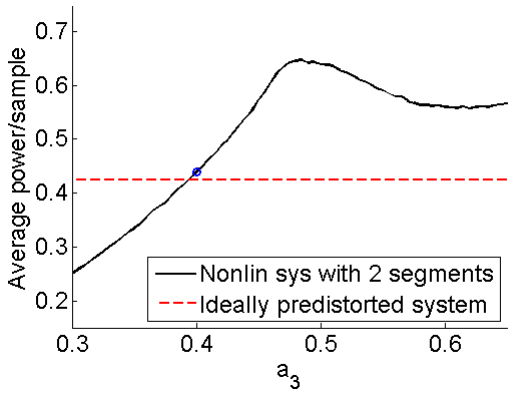

Figure 4.12: Average transmitted powers for an ideally predistorted system (dotted red) and nonlinear systems, using various 2-segments weight coefficients (black). Transmitted PSD is restricted by the topical mask.

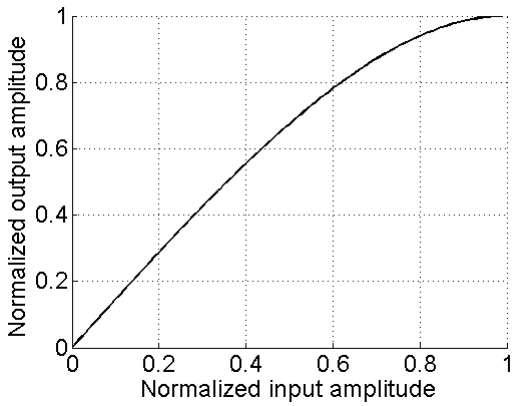

Figure 4.13: 2-segments, B-spline nonlinear characteristic, where $a_1 = 0.485$

4.3 Restricting the PSD with the BGAN Spectral Mask

The BGAN spectral mask is briefly presented in Chapter 3.2, and is illustrated in Figure 3.4. This mask is based on four different thresholds given at four different frequency values ($f1 - f4$), and the spectral distances between these are given in [12]. In this thesis, we only consider normalized frequencies, so $f1$ has been set to $(1+\alpha)/(2T)$ while $f2-f4$ was calculated from $f1$ by means of [12]. Linear curves were then drawn between the known values, resulting in the BGAN spectral mask.

When utilizing the simple mask, we calculated both the peak and the sidelobe level by averaging to minimize statistical variations, and then used the difference to see whether the PSD exceeded a mask constraint of Δp dB. As for the implementation of the BGAN mask, this has been done in a more simple fashion; The PSD has been estimated as described in Chapter 3.4, and the maximal value in the peak has been calculated. The BGAN spectral mask has then been placed on top of the transmitted PSD, with the peak of the mask equal to the peak of

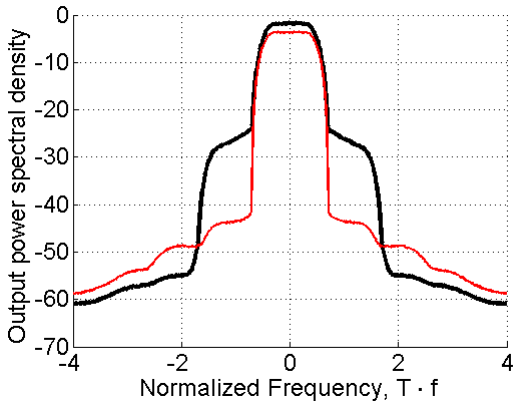

Figure 4.14: The transmitted PSD, restricted by the topical mask, of an ideally predistorted system (red) and a nonlinear system, with 2-segments where $a_1 = 0.485$.

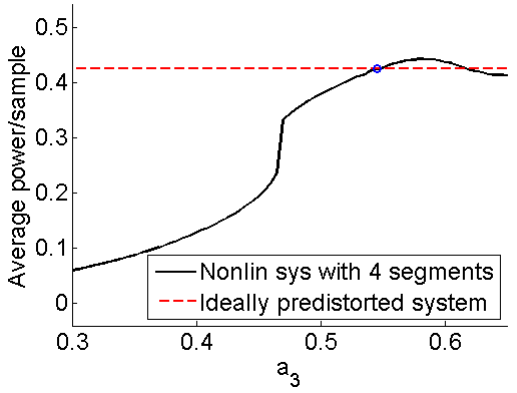

Figure 4.15: Average transmitted powers for an ideally predistorted system (dotted red) and nonlinear systems, using various 4-segments weight coefficients (black). Transmitted PSD is restricted by the topical mask.

the transmitted PSD. If the PSD for any frequency values exceeded the mask, the transmitted PSD was not accepted, and a new estimated PSD was calculated using more attenuation prior to the nonlinearity.

Thus, this model is more vulnerable for statistical variations as every point in the PSD have influence on whether or not we accept the transmitted signal in relevance to the mask. Hence, the results presented here will not be as reliable as those obtained when considering the transmitted PSD with respect to the simple mask constraints.

4.3.1 An Ideally Predistorted System

The ideally predistorted system is the same as the one we considered when using the simple mask constraints. Table 4.4 summarizes the most important results from this scenario, and Figure 4.17 illustrates the estimated transmitted PSD of this case. These results alone are not

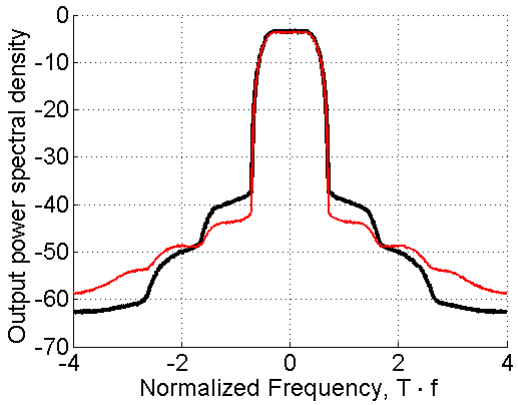

Figure 4.16: The transmitted PSDs, restricted by the topical mask, of an ideally predistorted system (red) and a nonlinear system, with 4-segments where $a_1 = 0.58$.

Measured variable	*Estimated Value*
Average transmitted power, $\bar{P}_{avg}$	0.5931 [Normalized]
Standard deviation, $\bar{S}_{Pavg}$	0.0002 [Normalized]
IBO, linear/dB	0.817 [Linear]/-0.8778 [dB]

Table 4.4: Estimated parameters for an ideally predistorted, restricted by the BGAN mask

very informative. However, when these results are used as a basis when examining the different nonlinear systems, it will become clear whether or not an ideally predistorted system is the optimal solution as regards transmitted power, when restrictions are placed by the BGAN mask.

4.3.2 Nonlinear Systems

This presentation of different nonlinear systems will follow the same outline as when we considered nonlinear systems restricted by the simple mask.

Fixed Coefficients in the Nonlinearities

Figure 4.18 illustrates the average transmitted power as a function of K. We observe that this function resembles the one presented in Figure 4.3. As mentioned, the results obtained here are less reliable than the results presented for the simple mask. However, they provide us with an idea of what happens when these nonlinearities are used in place of a linear element, which is worse performance when a small number of segments are used, and approximately equal performance when a larger number of segments are used. This was also the result we obtained when examining fixed nonlinearities with regard to a simple mask in the vicinity of the first sidelobe level.

By examining the different PSDs for these particular nonlinearities (Figure 4.19), we can observe that the actual limitation for all nonlinearities, as well as the ideally predistorted sys-

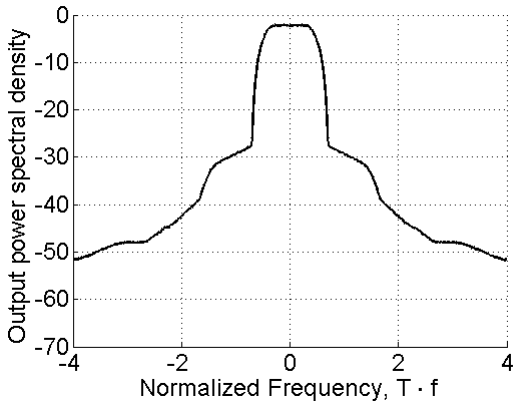

Figure 4.17: Transmitted PSD of the ideally predistorted system, restricted by the BGAN mask

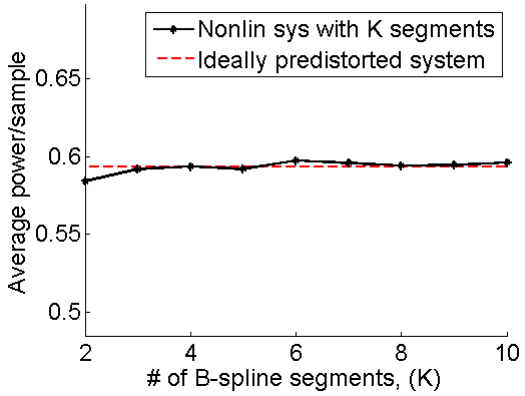

Figure 4.18: Average transmitted powers for an ideally predistorted system (dotted red) and nonlinear systems, using fixed weight coefficients (black). Transmitted PSD is restricted by the BGAN spectral mask.

tem, lies in the proximity of $1.35/T$. Thus, the examination has so far proved that restrictions placed by the BGAN mask is very alike to placing restrictions with a simple mask close to the mainlobe.

Two Segments Nonlinearities with One Degree Of Freedom

Figure 4.20 illustrates the average transmitted power for this considered set of nonlinearities. Once more, we observe that this resembles the results we obtained when restricting the transmitted PSD with a simple mask close to the mainlobe, and we can easily observe that the power efficiencies of the considered set of nonlinear systems, do not exceed that of an ideally predistorted system.

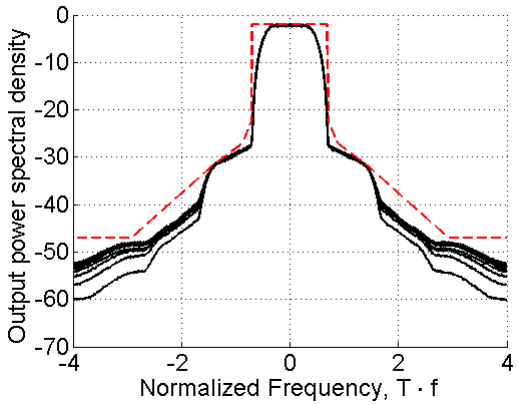

Figure 4.19: Transmitted PSDs of all considered nonlinear systems with fixed coefficients (black), seen in relation to the BGAN spectral mask (dotted red)

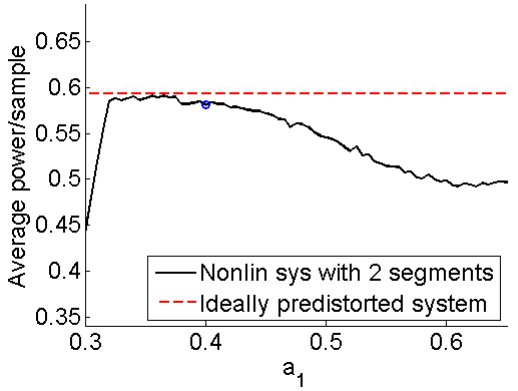

Figure 4.20: Average transmitted powers for an ideally predistorted system (dotted red) and nonlinear systems, using various 2-segments weight coefficients (black). Transmitted PSD is restricted by the BGAN spectral mask.

Four Segments Nonlinearities with One Degree Of Freedom

Once again, we obtain similar results as those obtained when placing restrictions on the transmitted PSD, with a simple mask close to the mainlobe. Figure 4.21 illustrates the average transmitted powers for the topical nonlinear systems, compared to an ideally predistorted system. We notice that several of the nonlinear system, utilizing an a_3 weight coefficient in the range of $0.52-0.55$, are approximately as power efficient as an ideally predistorted system. However, neither of these nonlinear system will outperform an ideally predistorted system.

4.3.3 Important Observations

We observed that none of the considered nonlinear systems here, restricted by the BGAN mask, were able to outperform an ideally predistorted system as regards transmitted power.

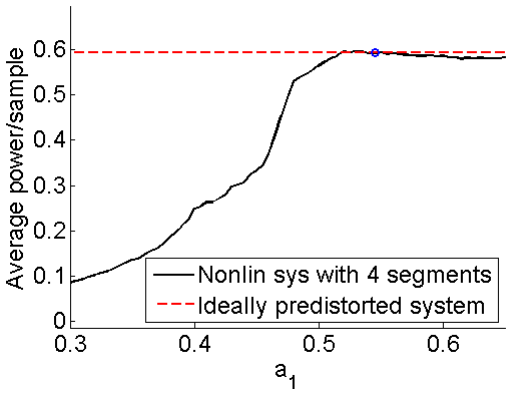

Figure 4.21: Average transmitted powers for an ideally predistorted system (dotted red) and nonlinear systems, using various 4-segments weight coefficients (black). Transmitted PSD is restricted by the BGAN spectral mask.

In the light of these observations, we conclude that an ideally predistorted is the optimal solution when the transmitted PSD is restricted with a BGAN mask.

Chapter 5

Conclusions

5.1 Conclusions and Main Findings

In this thesis, we have examined whether any of the nonlinear transmission systems considered were capable of outperforming an ideally predistorted system, as regards average transmitted power, when their PSDs were all restricted by the same spectral mask. To perform this examination, we simulated a simple baseband transmission system utilizing different nonlinear elements. For all considered nonlinear elements, we calculated the transmitted PSD of the system and examined whether it fulfilled the particular spectral mask. When the restrictions in transmitted PSD were fulfilled, an estimate of the average transmitted power was computed and stored for further use. All esimates, restricted by the same spectral mask, were then compared to the average transmitted power of an ideally predistorted system.

The main findings presented in this report can be summarized as follows. First, the nonlinearities considered have a huge impact on the first sidelobe level. Consequenctly, when restrictions are placed by means of the BGAN mask [12] or a simple mask at the first sidelobe level, the ideally predistorted system has proved to be optimal, as regards transmitted power. When a simple mask constraint is utilized outside the first sidelobe level, several of the nonlinear systems do obtain higher average transmitted power than an ideally predistorted system, with a 2-segments B-spline nonlinearity[1] as the optimal solution of those considered.

We thus conclude that as long as limitations are placed on the sidelobe level close to the mainlobe, an ideally predistorted system is the obvious choice. On the other hand, should no such limitations exist within the first sidelobe, a nonlinear system has proven to obtain higher transmitted power. Hence, such a transmitter could be considered when designing the system.

5.2 Future Work

In this thesis, we have only considered a particular set of nonlinearities in relevance to a basic baseband transmission system. Suggestions for further work on this subject are:

[1] Utilizing [0.485 0.7575 0.485] as weight coefficients

- Find the optimal nonlinearity by using numerical optimization of all parameter B-splines with a larger number of intervals.
- Use an analytical approach to spectral estimationan because a numerical calculation of the PSD is time consuming.

Bibliography

[1] John G. Proakis and Dimitris G. Monolakis. *Digital Signal Processing - Principles, Algorithms and Applications.* Prentice-Hall Inc, New Jersey, 1996. 2.1, 2.1.1, 2.1.1, 2.1.2, 2.3.2

[2] Nima Safari, Nils Holte, and Terje Røste. Digital predistortion of power amplifiers based on spline approximation of the amplifier characteristics. *Vehicular Technology Conference, IEEE 66th*, pages 2075–2080, 2007. 2.2, 3.1

[3] Adel A. M. Saleh. Frequency-independent and frequency-dependent nonlinear models of twt amplifiers. *IEEE Transaction on communications, VOL. COM-29, NO. 11*, pages 1715–1720, 1981. 2.3

[4] Osamu Shimbo. *Transmission Analysis in Communication Systems, Volume 1.* Computer Science Press, Inc, Maryland, 1988. 2.3.2

[5] Erwin Kreyszig. *Advanced Engineering Mathematics 8th ed.* John Wiley & Sons Inc., New York, 1999. 2.3.2

[6] Lars Sundstrøm. *Digital RF Power Amplifier Linearisers.* PhD thesis, Department of Applied Electronics, Lund University, Sweden, 1995. 2.3.2, 3.1

[7] John R. Barry, Edward A. Lee, and David G. Messerschmitt. *Digital Communication.* Springer, New York, 2004. 3.1, 3.2, 3.4

[8] Aldo N. D'Andrea, Vincenzo Lottici, and Ruggero Reggiannini. Rf power amplifier linearization thorugh amplitude and phase predistortion. *IEEE Transaction on communications, VOL. 44, NO. 11*, pages 1477–1484, 1996. 3.1

[9] A.N.D'Andrea, V.Lottici, and R.Reggiannini. Efficient digital predistortion in readio relay links with nonlinear power amplifiers. *IEE Procedings online no. 20000358*, pages 175–179, 2000. 3.1

[10] Angelo Bernadini and Silvia De Fina. Analysis of diffeent optimization criteria for if predistortion in digital radio links with nonlinear amplifiers. *IEEE, Transactions on communications, VOL 45*, pages 421–428, 1997. 3.1

[11] Andrea Goldsmith. *Wireless Communications.* Cambridge University Press, New York, 2005. 3.2

[12] Broadband global area network (bgan) sdm volume 5 chapter 1. Inmarsat confidential paper. 3.2, 4.3, 5.1

[13] Simon Haykin. *Communication Systems, 4th edition.* John Wiley & Sons, Inc, New Jersey, 2001. 3.4

[14] Ronald E. Walpole, Raymond H. Myers, Sharon L. Myers, and Keying Ye. *Probability & Statistics for Engineers & Scientists.* Prentice Hall PTR, New Jersey, 2002. 3.4, 3.4

[15] Michel C. Jeruchim, Philip Balaban, and K. Sam Shanmugan. *Simulation of Communication Systems - Modelling, Methodology and Techniques.* Kluwer Academics/Plenum Publishers, New York, 2000. 3.5